iScience

CellPress
OPEN ACCESS

Article

Fus3 regulates asexual development and trap morphogenesis in the nematode-trapping fungus *Arthrobotrys oligospora*

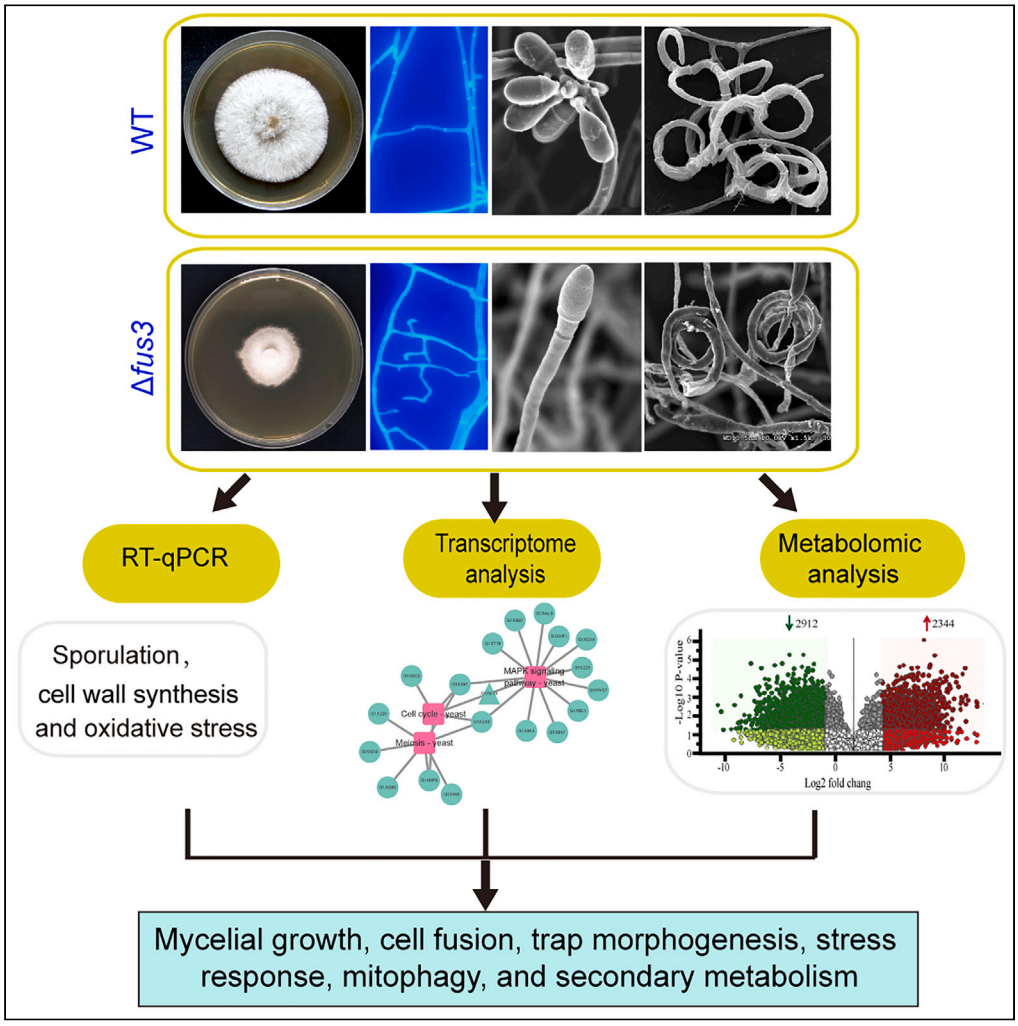

Meihua Xie, Na Bai, Xuewei Yang, Yankun Liu, Ke-Qin Zhang, Jinkui Yang

jinkui960@ynu.edu.cn

Highlights

Fus3 is required for cell fusion, trap morphogenesis, and nematocidal activity

Fus3 plays a crucial role in asexual growth, stress response, and secondary metabolism

Fus3 regulates DNA damage, mitochondrial morphology, and autophagy

Fus3 impairs diverse phenotypic traits by regulating downstream targets

Xie et al., iScience 26, 107404
August 18, 2023
https://doi.org/10.1016/j.isci.2023.107404

iScience

CellPress
OPEN ACCESS

Article

Fus3 regulates asexual development and trap morphogenesis in the nematode-trapping fungus *Arthrobotrys oligospora*

Meihua Xie,[1,2] Na Bai,[1] Xuewei Yang,[1] Yankun Liu,[1] Ke-Qin Zhang,[1] and Jinkui Yang[1,3,*]

SUMMARY

Mitogen-activated protein kinase (MAPK) Fus3 is an essential regulator of cell differentiation and virulence in fungal pathogens of plants and animals. However, the function and regulatory mechanism of MAPK signaling in nematode-trapping (NT) fungi remain largely unknown. NT fungi can specialize in the formation of "traps", an important indicator of transition from a saprophytic to a predatory lifestyle. Here, we characterized an orthologous Fus3 in a typical NT fungus *Arthrobotrys oligospora* using multi-phenotypic analysis and multi-omics approaches. Our results showed that Fus3 plays an important role in asexual growth and development, conidiation, stress response, DNA damage, autophagy, and secondary metabolism. Importantly, Fus3 plays an indispensable role in hyphal fusion, trap morphogenesis, and nematode predation. Moreover, we constructed the regulatory networks of Fus3 by means of transcriptomic and yeast two-hybrid techniques. This study provides insights into the mechanism of MAPK signaling in asexual development and pathogenicity of NT fungi.

INTRODUCTION

The mitogen-activated protein kinase (MAPK) cascade is a key intracellular signal sensor that transmits information using the phosphorylation/dephosphorylation cycle of proteins.[1] There are five MAPK pathways in *Saccharomyces cerevisiae*, which are involved in the regulation of mating, invasive growth, cell-wall integrity, and ascospore formation.[2] In the MAPK Fus3/Kss1 cascades pathway, extracellular pheromones bind to cell surface receptors, triggering a series of intracellular signaling responses. This MAPK cascade pathway is mainly involved in regulating the cell-to-cell communication, cell fusion, appressorium development, pathogenicity, and secondary metabolism of pathogenic fungi.[2,3] For example, Fus3 and orthologs are required for the completion of cell fusion in *S. cerevisiae* and *Neurospora crassa*,[4,5] the yeast MAPK Fus3 mediates sexual cell fusion, whereas the Fus3 ortholog (MAK-2) mediates vegetative (asexual) cell fusion in *N. crassa*. In *Botrytis cinerea*, Bmp1 (homologous to Fus3) is essential for plant infection, and the mutant produced normal conidia and mycelia, and was nonpathogenic for carnation flowers and tomato leaves.[6] This pathway is also required for pathogenicity in *Claviceps purpurea* and *Stagonospora nodorum*.[7] In *Magnaporthe grisea*, Pmk1 (homologous to Fus3) regulates appressorium formation, and is required for penetration of the host epidermis and infection growth.[8] In *Aspergillus nidulans*, MpkB (homologous to Fus3) plays a role in mycelial growth, conidia, conidial viability, sexual development, and autolysis.[9] Fus3-Kssl-like MAPK genes in *Pyrenophora teres*[10] and *Cochliobolus heterostrophus*[11] affect conidiation. Furthermore, Fus3 regulates the production of secondary metabolites in several species of *Aspergillus*, such as *A. fumigatus*,[12] *A. flavus*,[13–15] and *A. nidulans*.[16,17] These findings suggest that Fus3 plays an important role in vegetative and sexual cell-cell fusion, fungal growth, development, secondary metabolism, and pathogenicity.

Nematode-trapping (NT) fungi are carnivorous microbes that can produce different types of trapping devices (traps) to prey on nematodes.[18] NT fungi can live a saprophytic life, but when there are inducers such as nematodes in the environment, their vegetative hyphae are specialized to form unique traps, and their lifestyle changes from the saprophytic stage to the parasitic stage.[19,20] *Arthrobotrys oligospora* is a model NT fungus for studying the interaction between fungi and nematodes, and can produce adhesive three-dimensional hyphal networks to prey on nematodes.[21] The mature hyphal networks consist of 5–8 mycelial loops, and the formation of the traps is the result of the branching, bending and fusion of the hyphae, and is

[1]State Key Laboratory for Conservation and Utilization of Bio-Resources, Key Laboratory for Microbial Resources of the Ministry of Education, School of Life Sciences, Yunnan University, Kunming 650091, P.R. China

[2]School of Resource, Environment and Chemistry, Chuxiong Normal University, Chuxiong 675000, P.R. China

[3]Lead contact

*Correspondence: jinkui960@ynu.edu.cn

https://doi.org/10.1016/j.isci.2023.107404

also a prerequisite for *A. oligospora* and other NT fungi to capture the nematodes.[22] The formation of traps is a complex process in which multiple pathways such as cell wall biosynthesis, signal transduction pathways, and peroxisomal protein synthesis are involved.[23]

In recent years, increasing studies have demonstrated that heterotrimeric G-proteins (G-protein) and related signaling pathways play a crucial role in the mycelia growth, trap formation, and pathogenicity of NT fungi, such as *A. oligospora*.[24–28] For example, deletion of the G-protein β-subunit-encoding gene nearly abolished trap formation[24]; and the cAMP-PKA signaling regulated hyphal growth, conidiation, trap morphogenesis, stress tolerance, and autophagy.[28] In addition, deletion of *hog1* resulted in hypersensitivity to hyperosmolarity, defective conidia formation, and reduced trap formation and predation efficiency.[29] Similarly, with disruption of the three components (AoBck1, AoMkk1 and AoSlt2) of the cell-wall integrity MAPK cascade, all of the Δ*Aobck1*, Δ*Aomkk1*, and Δ*Aoslt2* mutants showed severe defects in vegetative growth, and lost the ability to produce mycelial traps for nematode predation.[30,31] Recently, an orthologous Fus3 was identified in *A. oligospora* (strain TWF154), where deletion of *fus3* abolished nematode-induced trap morphogenesis and impaired the growth of hyphae.[32] However, the function and related regulatory network of Fus3 remain largely unknown in *A. oligospora* and other NT fungi.

In this study, we characterized an orthologous Fus3 in *A. oligospora* (strain ATCC24927) using multi-phenotypic analysis and multi-omics approaches. Surprisingly, we found that the Δ*fus3* mutant could not produce three-dimensional networks, but rather a specialized spiral hyphal coil, due to the abolishment of hyphal fusion, which is different from previous report[32]; meanwhile, the absence of *fus3* caused a severe defect in conidiophore development, stress response, DNA damage, mitochondrial morphology, and secondary metabolism. In addition, we probed the regulatory networks and interacting proteins of Fus3 using transcriptomic and yeast two-hybrid (Y2H) techniques. Our results suggest that Fus3 plays an important role in asexual development, stress response, cell fusion, pathogenicity, mitochondrial development, DNA damage, and secondary metabolism.

RESULTS

Sequence analysis of Fus3

The orthologous *fus3* gene was retrieved from the fungus *A. oligospora*, which encodes a 350-amino acid polypeptide with a predicted molecular mass of 40.66 kDa and an isoelectric point of 6.90. Phylogenetic analysis indicated that Fus3 orthologs from several NT fungi (*A. oligospora*, *Drechslerella stenobrocha*, *Dactylellina haptotyla*, and *Arthrobotrys flagrans*) were clustered in a single clade (Figure S1A). Sixteen Fus3 orthologs from different fungi all contained active sites of Ser/Thr protein kinase (IPR008271) and protein kinase domain (IPR000719) (Figure S1B). Furthermore, Fus3 showed a high similarity (more than 89.7%) to other fungal orthologs, apart from *S. cerevisiae*, while it shared a similarity of 60.3% with *S. cerevisiae* (Figure S1C).

Fus3 regulates mycelial growth, cell nucleus number, and endocytosis

The gene *fus3* was disrupted by a homologous recombination strategy, and transformants were verified by PCR with primers yz*fus3*-5f and yz*fus3*-3r and Southern blotting with the restriction enzyme *Stu*I (Table S1; Figures 2A–2C). The gene *fus3* was disrupted by a homologous recombination strategy, and transformants were verified by PCR with primers yz*fus3*-5f and yz*fus3*-3r (Table S1; Figures S2A and S2B). Subsequently, the genomic DNA of the wild-type (WT) and corresponding transformants was digested with the restriction enzyme *Stu*I and used in Southern blotting analysis, and a single band of the expected size appeared in the WT and Δ*fus3* mutant strains (Figure S2C). Finally, we obtained two positive transformants (Δ*fus3*-71 and Δ*fus3*-72).

Compared with WT, the mycelial growth rate of the Δ*fus3* mutant was remarkably decreased on the PDA, tryptone-glucose agar (TG), and tryptone yeast-extract glucose agar (TYGA) media, and Δ*fus3* mutant exhibited a reduction in the number of aerial mycelia (Figures 1A and 1B). The hyphae of the Δ*fus3* mutant contained more hyphal septa than WT hyphae, and some hyphae also swelled and deformed (Figures 1C and 1D). The hyphal cells of the Δ*fus3* mutant had a reduced number of nuclei compared to WT (Figures 1E and 1F). To probe whether Fus3 plays a role in endocytosis, we stained the fungal hyphae with the lipophilic styryl dye FM4-64, after 10 min of staining with the lipophilic styryl dye FM4-64, the WT hyphal cells were filled with the dye solution, whereas only the membrane portion of the hyphal cells in the Δ*fus3* mutant was stained (Figure 1G). Further observation by transmission electron microscopy (TEM) also found that the WT contained more endocytic structures than the Δ*fus3* mutant (Figure 1H).

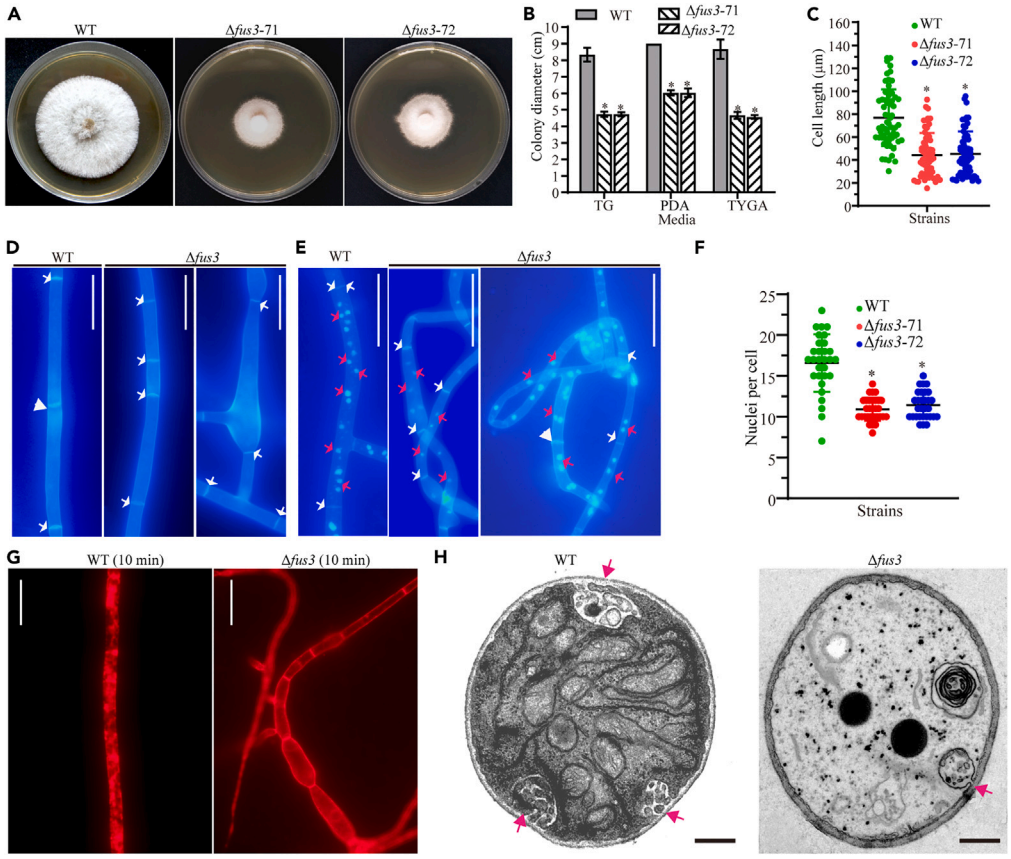

Figure 1. Comparison of mycelial growth, morphology, septa, cell nuclei, and endocytic structures in WT and Δ*fus3* mutants

(A) The colony morphology after growth on TYGA plate at 28°C for 5 days.

(B) Colony diameters of WT and Δ*fus3* mutant strains after growth on TG, PDA, and TYGA plate for 7 days.

(C) Comparison of mycelial cell length of the WT and Δ*fus3* mutant strains. Error bars: SD from 61 replicates.

(D) Mycelial morphology after culturing on CMY plate for 7 days and staining with 20 μg/mL calcofluor white (CFW). Arrows point to hyphal septa. Scale bar: 10 μm.

(E and F) Nuclei in WT and Δ*fus3* mutant hyphae were visualized after staining with CFW and DAPI. White and pink arrows indicate septa and nuclei, respectively. Scale bar: 10 μm.

(G) Mycelia of WT and Δ*fus3* mutant strains were stained with FM4-64 at 10 min. Scale bar: 10 μm.

(H) The endocytic structures in WT and Δ*fus3* mutants were observed using transmission electron microscopy. Arrows point to hyphal endocytic structures. Scale bar: 0.5 μm. Error bars in (B, C, and F): Data are represented as mean ± SD. The asterisk in (B, C, and F) indicates a significant difference between mutants and the WT strain (Tukey's HSD, $p < 0.05$).

Fus3 regulates conidiophore morphology and conidia yield

Deletion of *fus3* resulted in a significant reduction in the number of conidiophores compared to the WT (Figure 2A), and a corresponding reduction in conidiation, which was reduced by approximately 99.5% (Figure 2B). In addition, the apex of the WT conidiophores had multiple conidia (1–16), while the apex of the Δ*fus3* mutant conidiophores only had one or two conidia (Figure 2C). This reduction in conidiation of the mutant is likely a combination of less conidiophores and less conidia per conidiophore. At the same time, 90.8% ± 2.2 of the conidia in the Δ*fus3* mutant changed remarkably in morphology (Figure 2D). In addition, the number of nuclei in the Δ*fus3* mutant (9–17 nuclei in each conidium) conidia was reduced compared with the WT strain (10–26 nuclei per conidium) (Figures 2E and 2F). The transcription of eight putative sporulation-related genes (*abaA*, *aspB*, *flbC*, *fluG*, *nsdD*, *rodA*, *velB*, and *vosA*)[33] between the WT and Δ*fus3* mutant strains was determined using real-time quantitative PCR (RT-qPCR) at different growth stages. Compared with WT, both *rodA* and *abaA* were downregulated at three time points, and *abaA* was the most remarkably downregulated (Figure 2G).

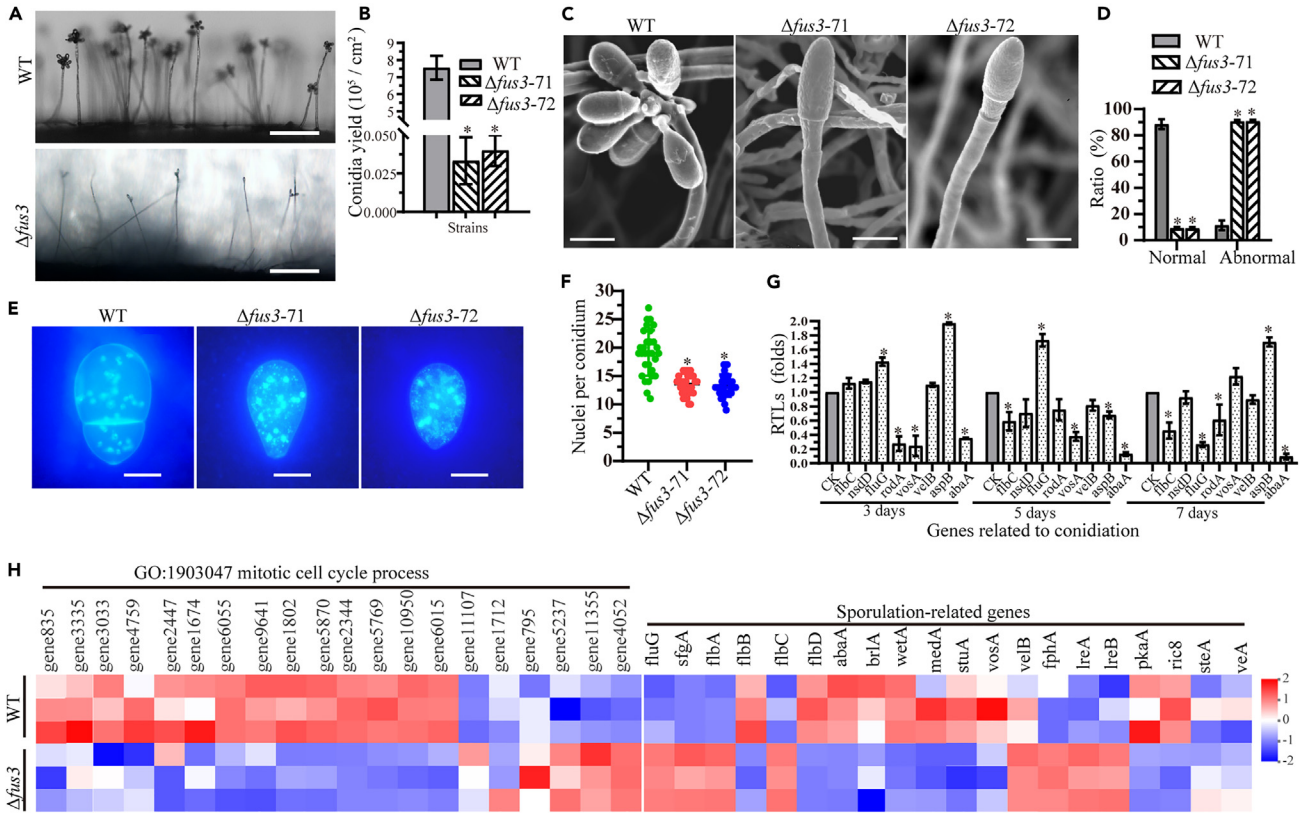

Figure 2. Comparison of conidial production and conidiophore morphology between the WT strain and Δ*fus3* mutants

(A) Conidiophores of WT strains and Δ*fus3* mutants were observed by light microscopy. Bar: 100 μm.

(B) Conidial yields of the WT strain and Δ*fus3* mutants.

(C) Morphology of conidiophores and spores. Bar: 10 μm.

(D) Comparison of morphologically normal and abnormal spores in the WT strain and Δ*fus3* mutants.

(E) Conidial morphology and nuclei were visualized by CFW and DAPI staining. Bar: 5 μm.

(F) The number of nuclei in spores.

(G) Relative transcription levels (RTLs) of sporulation-related genes in Δ*fus3* in the mutant and WT strain at different time points.

(H) Heatmap of gene expression involved in the mitotic cell cycle process and sporulation in WT and Δ*fus3* mutant strains.

Error bars in (B, D, F, and G): Data are represented as mean ± SD. The asterisk in (B, D, F, and G) indicates a significant difference between mutants and the WT strain (Tukey's HSD, $p < 0.05$).

To probe the influence of Fus3 on mitotic process and conidiation, we compared the transcriptional levels of genes involved in mitotic cell cycle process and conidiation between the Δ*fus3* mutant and WT strain by RNA-sequencing. Analysis of clustering heatmaps showed that 16 genes involved in mitotic cell cycle process were upregulated and four were downregulated, such as DNA-repair protein Rad2 (AOL_s00007g552), serine/threonine protein kinases Ar1 (AOL_s00043g508) and Chk1 (AOL_s00080g44) were upregulated, while actin-related protein 2/3 complex subunit 1A (AOL_s00076g149) was downregulated. There were 15 putative sporulation-related genes upregulated and five downregulated, including upregulation of *flbA*, *fluG*, *flbB*, and *flbC*, and downregulation of *flbD*, *abaA*, *stuA*, *vosA*, and *veA* (Figure 2H; Tables S2 and S3).

Fus3 regulates multiple stress responses

The mycelial growth of the WT and Δ*fus3* mutant strains was inhibited on TG medium supplemented with osmotic agents (NaCl and sorbitol), oxidants (H_2O_2 and menadione), and cell wall-disturbing agents (Congo red and SDS) (Figure 3A). The influence of these stressors on the WT and Δ*fus3* mutant strains was determined by relative growth inhibition (RGI).[34] After exposure to 0.25 M sorbitol, the RGI value of the Δ*fus3* mutant increased by 25.4%, compared to that of the WT strain. Similarly, the RGI value, after exposure to 0.05 mM menadione and 5 mM H_2O_2, increased by 27.7 and 48.2%, respectively. The RGI value,

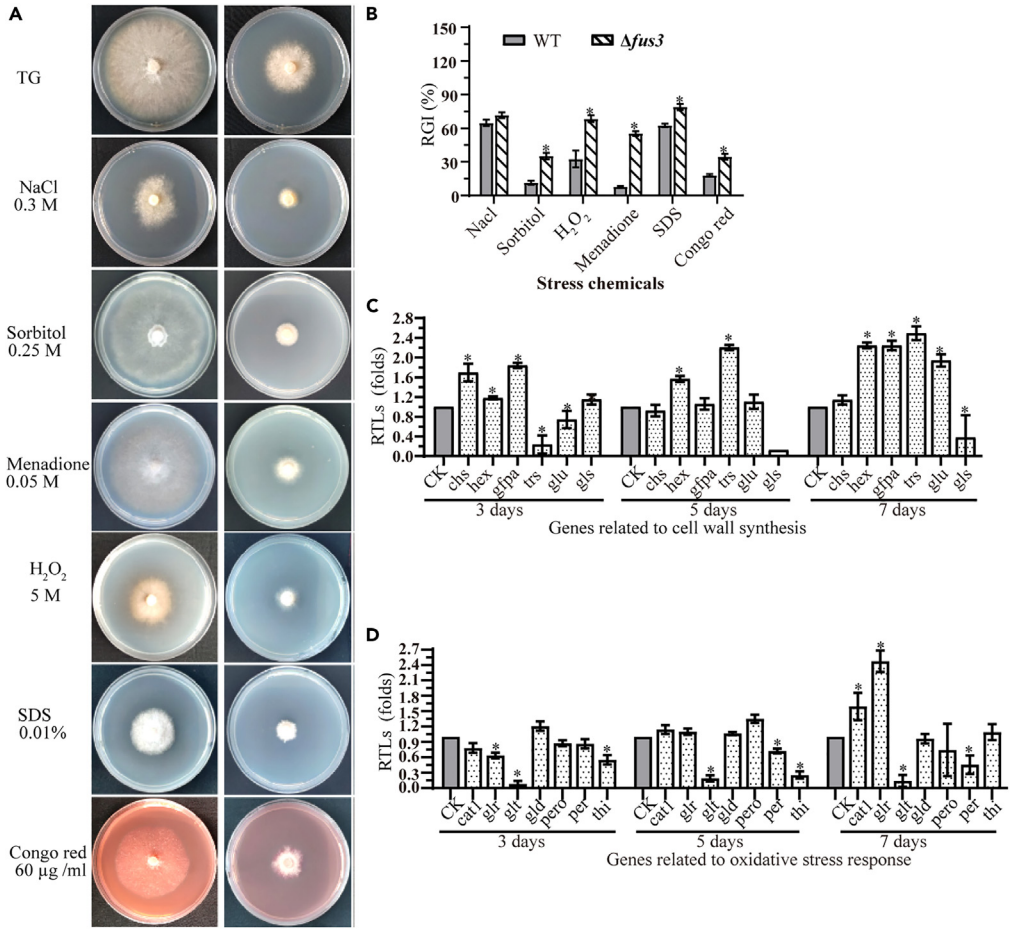

Figure 3. Chemical stress tolerance of WT and Δ*fus3* mutants

(A) Colonial morphology of fungal strains treated with chemical stressors.

(B) Relative growth inhibition (RGI) of fungal colonies grown on TG plates supplemented with different chemicals.

(C) Relative transcription levels (RTLs) of genes involved in cell wall biosynthesis in Δ*fus3* mutants and WT strain at different time points.

(D) RTLs of genes involved in oxidative stress response in Δ*fus3* mutants and WT strain at different time points.

Error bars in (B–D): Data are represented as mean ± SD. The asterisk in (B–D) indicates a significant difference between mutants and the WT strain (Tukey's HSD, $p < 0.05$).

after exposure to 0.01% SDS and 60 μg/mL Congo red, increased by 14.6 and 16.0%, respectively (Figure 3B). The cell wall synthesis-related gene *gls* was remarkably downregulated in the Δ*fus3* mutant on days 5 and 7 compared to WT, whereas *hex*, *gfpa*, *trs*, and *glu* were significantly upregulated on day 7 (Figure 3C). In addition, the transcriptional levels of seven genes associated with oxidative stress response were compared between the WT and Δ*fus3* mutant strains by RT-qPCR, and the glutathione S-transferase (*glt*) gene was downregulated in Δ*fus3* mutant at three time points compared with WT strains, while *cat1* and *glr* were significantly upregulated on day 7 (Figure 3D).

Fus3 regulates hyphal fusion, trap morphogenesis, and pathogenicity

Hyphal fusion can be observed in the WT strain during spore germination and vegetative growth, whereas hyphal fusion is abolished in the Δ*fus3* mutant, and the hyphae are coiled (Figures 4A and 4B). Woronin bodies (WBs) are a specialized class of peroxisome-derived organelles that quickly plug the septal pore upon injury of the hypha, avoiding the excessive loss of cytoplasm.[35] Further TEM observation of the hyphae showed that the septal pores of the WT hyphae were sealed with WBs, whereas about 50% septal pores of the Δ*fus3* mutant were not sealed with WBs (Figure 4C). In addition, the traps produced by the WT and Δ*fus3* mutant strains were observed by means of scanning electron microscopy (SEM) after

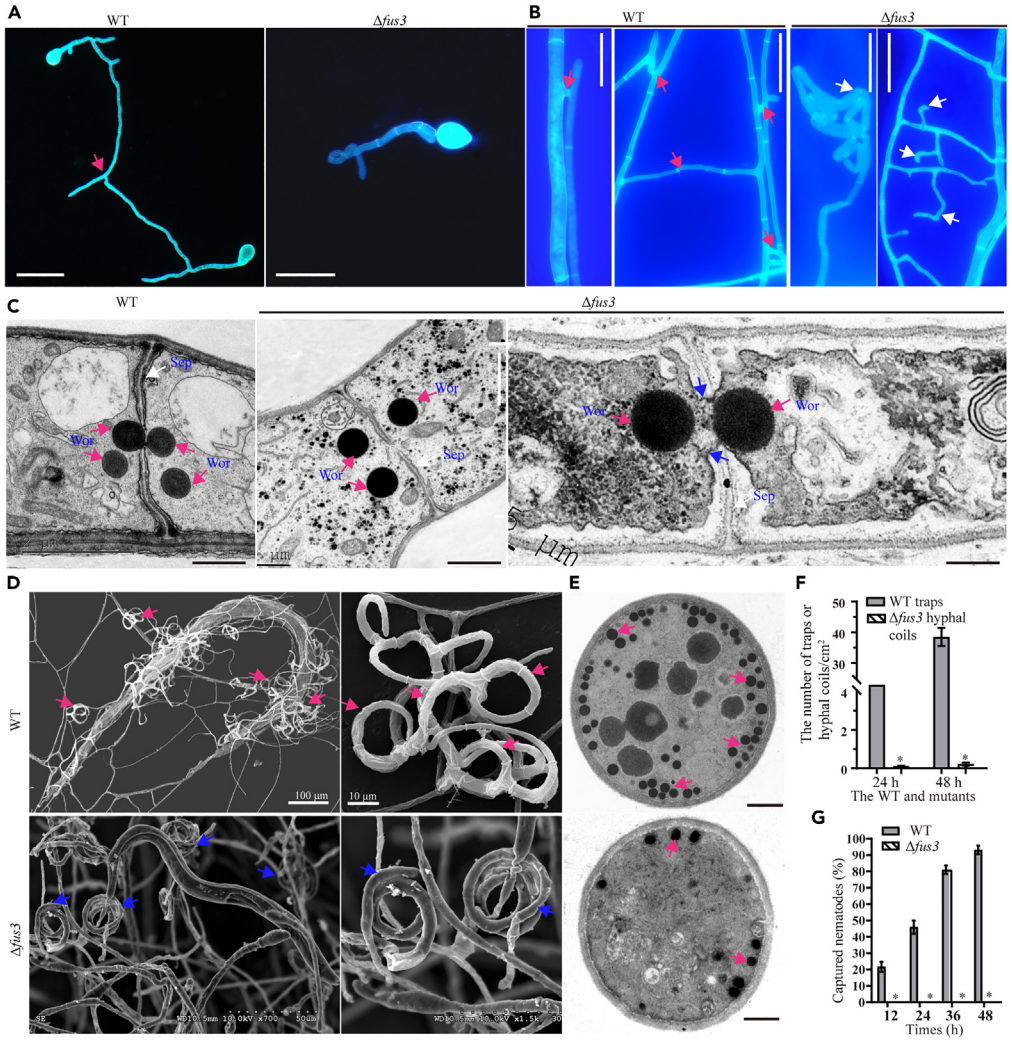

Figure 4. Comparison of hyphal fusion, trap formation, and nematocidal activity of WT and Δ*fus3* mutants

(A) Spore germination after 48 h post incubation and stained with calcofluor white and then observed with a microscope. Pink arrows indicate hyphal fusion. Bar: 20 μm.

(B) Mycelial morphology of WT and Δ*fus3* mutants cultured on PDA medium at 28°C for 7 days. Pink arrows indicate hyphal fusion, white arrows indicate hyphal physical contact or hyphal branching of the Δ*fus3* mutants. Bar: 20 μm.

(C) Woronin bodies in the hyphal cells of WT and Δ*fus3* mutant strains were observed by TEM. White, pink, and blue arrows point toward the hyphal septum, Woronin body, and connected cytoplasm, respectively. Bar: 1 μm.

(D) Comparison of trap morphology after being induced with nematodes for 48 h by SEM and TEM. Pink and blue arrows point toward the traps and hyphal coils, respectively.

(E) Trap cells of WT and Δ*fus3* mutants were observed by TEM. Pink arrows point toward ED bodies. Bar: 0.5 μm.

(F) Traps produced at 24 and 48 hpi.

(G) Percentages of nematodes captured by WT and Δ*fus3* mutant strains at different time points.

Error bars in (F and G): Data are represented as mean ± SD. The asterisk in (F and G) indicates a significant difference between mutants and the WT strain (Tukey's HSD, $p < 0.05$).

induction with nematodes for 48 h, and the WT strain produced many traps containing multiple mycelial loops through hyphal fusion, and most of the added nematodes were captured and digested. However, the Δ*fus3* mutant was not able to produce typical traps, instead producing a small number of hyphal coils due to the abolishment of hyphal fusion, and only few nematodes were captured. In addition, TEM observation showed that the WT trap cells contained many electron-dense (ED) bodies, whereas the number of ED bodies in the Δ*fus3* hyphal cells was significantly reduced (Figure 4D). Further comparison of the traps produced by the WT and the hyphal coil produced by the Δ*fus3* mutant showed that the WT produced 13.5

and 38.5 traps per cm^2 at 24 and 36 h post induction (hpi), respectively, whereas the Δ*fus3* mutants only produced 0.1 and 0.2 hyphal coils per cm^2 at 24 and 36 hpi, respectively (Figure 4E). Correspondingly, the nematode predation rate of the WT reached 21.7%, 45.9%, 81.1% and 93.1% at 12, 24, 36 and 48 hpi, respectively, whereas the nematode predation ability of the Δ*fus3* mutant was almost abolished at 12, 24 and 36 hpi, and only about 3.9% of the nematodes were captured at 48 hpi (Figure 4F).

Fus3 regulates DNA damage repair and mitophagy

The terminal deoxynucleotidyl transferase-mediated dUTP nick end-labeling (TUNEL) assay revealed increased DNA fragmentation in the hyphae and spores of the Δ*fus3* mutant compared with that in those of the WT strain (Figures 5A–5C). TEM observation revealed that mitochondria were deformed in the Δ*fus3* mutant (Figure 5D), and the expression levels of mitochondrial distribution and morphology proteins (MD342 and MDM10)[36] were upregulated compared with WT (Figure 5E). Under starvation conditions, TEM observation showed that some autophagosomes were distributed in the hyphal vacuoles of WT, whereas the vacuoles of the Δ*fus3* mutant were larger than those of WT, and there was mitophagy in the vacuoles (Figure 5F). In addition, an analysis of clustering heatmaps revealed that the transcription of genes involved in autophagy and mitophagy was remarkably altered between the WT and the Δ*fus3* mutant strains, with 24 genes being upregulated and 14 genes being downregulated in autophagy, whereby vacuolar protein sorting proteins VpsB (AOL_s00215g592) and DigA (AOL_s00215g688) and cAMP-dependent protein kinase (AOL_s00054g80) were upregulated, while inositol hexaphosphate kinase Kcs1 (AOL_s00215g763), serine proteases (AOL_s00170g103), and serine proteinase PepC (AOL_s00004g122) were downregulated. In mitophagy, 31 genes were upregulated, and 12 genes were downregulated, with mitochondrial inheritance component Mdm12 (AOL_s00193g178), DNA polymerase gamma (AOL_s00215g177), and mitochondrial outer membrane protein Mdm10 (AOL_s00076g313) being upregulated, while small nuclear ribonucleoprotein D3 (AOL_s00215g169), protein phosphatase 2C (AOL_s00097g512), and autophagy-related protein 11 (AOL_s00004g301) were downregulated (Figure 5G; Tables S4 and S5).

Transcriptomic insights into the regulatory role of Fus3

Transcriptional profiles of WT and Δ*fus3* mutant strains were compared on the basis of RNA sequencing. Quality control alignment of sequencing data and statistical analysis of sequence alignment showed that there was no contamination in related experiments, and the genes in each group were effectively expressed (Table S6). Principal component analysis showed that deletion of *fus3* resulted in different gene expression patterns between the WT and the Δ*fus3* mutant strain (Figure S3). During vegetative growth, the Δ*fus3* mutant had 2,200 and 1,564 differentially expressed genes (DEGs) compared to the WT strain, respectively (Figure 6A). Gene Ontology (GO) enrichment of the above DEGs found that the upregulated DEGs were mainly involved in biological processes such as RNA processing, proteasomal protein catabolic process, actin polymerization or depolymerization, DNA-directed 5′-3′ RNA polymerase activity, positive regulation of RNA metabolic process, maturation of SSU-rRNA, glucan biosynthetic process, integral component of nuclear inner membrane, and integral component of organelle membrane. The downregulated DEGs were mainly involved in processes such as glucose metabolic processes, carboxylic acid catabolic processes, metal ion transport, translation, nucleoside metabolic processes, cytoplasmic translation, negative regulation of apoptotic processes, ribonucleotide metabolic processes, and propionate metabolic processes (Figure 6B; Table S7). Further Kyoto Encyclopedia of Genes and Genomes (KEGG) enrichment showed that compared to WT, the Δ*fus3* mutant exhibited alterations in protein synthesis and processing (ribosome, RNA transport, and protein export), energy (glycolysis/gluconeogenesis, citrate cycle, and glyoxylate and dicarboxylate metabolism), autophagy processes (autophagy, mitophagy, and phagosome), oxidative phosphorylation, MAPK signaling, cell cycle, endocytosis, peroxisome, and proteasome (Figure S6C).

During the trap formation and nematode predation stages, the transcription level of the Δ*fus3* mutant at each time point changed significantly compared with WT, that is, the Δ*fus3* mutant had 1984, 1974, and 1917 upregulated and 2082, 1733 and 1271 downregulated genes at 12, 24, and 36 hpi, respectively (Figure 7A). In addition, the Δ*fus3* mutant had 41.8% (1698/4066), 26.2% (972/3707), and 23.5% (749/3188) DEGs at 12, 24, and 36 hpi in response to nematode challenge compared to WT, respectively. Among these DEGs, those related to the regulation of transcription DNA templates, intracellular protein transport, regulation of calcium ion transport, protein modification by small protein conjugation or removal, and phosphatidylinositol dephosphorylation were significantly enriched at 12 hpi; those involved in the purine

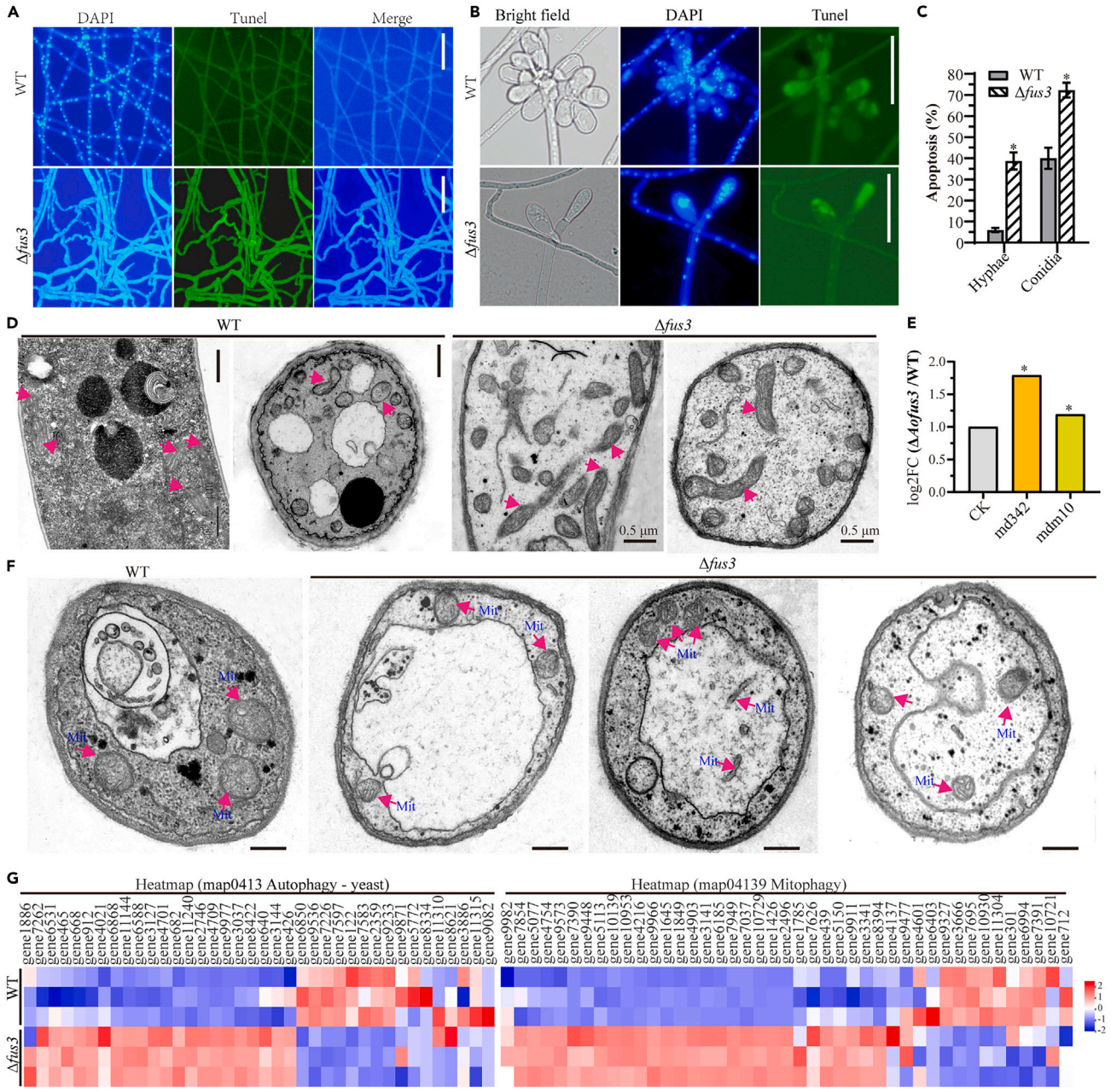

Figure 5. Comparison of DNA damage, mitochondrial morphology, and autophagy in WT and Δ*fus3* strains at the vegetative growth stage

(A) Hyphae of WT and Δ*fus3* strains grown on CMY medium at 28°C for 10 days were stained with DAPI and TUNEL. Bar: 20 μm.

(B) Conidia of WT and Δ*fus3* strains stained with DAPI and TUNEL and examined by fluorescence microscopy. Bar: 20 μm.

(C) Comparison of mycelial cells and conidial apoptosis in WT and Δ*fus3* strains (the data are presented as the mean ± SD from three independent experiments, *$p < 0.05$).

(D) Mitochondrial morphology in WT and Δ*fus3* mutant hyphal cells was observed by TEM. Pink arrows point toward mitochondria. Bar: 0.5 μm.

(E) Comparison of transcription of genes involved in mitochondrial membrane in WT and Δ*fus3* strains. Gene *md342* encodes mitochondrial distribution and morphology protein 342 and *mdm10* encodes mitochondrial distribution and morphology protein 10. CK indicates the standard (which has an RTL of 1) for the statistical analysis of the RTL of each gene in a deletion mutant compared to that in the WT strain (Tukey's HSD, *$p < 0.05$).

(F) TEM observations of autophagy in WT and Δ*fus3* strains. Pink arrows point toward mitochondria. Bar: 0.5 μm.

(G) Heatmap of gene expression involved in autophagy and mitophagy in WT and Δ*fus3* strains.

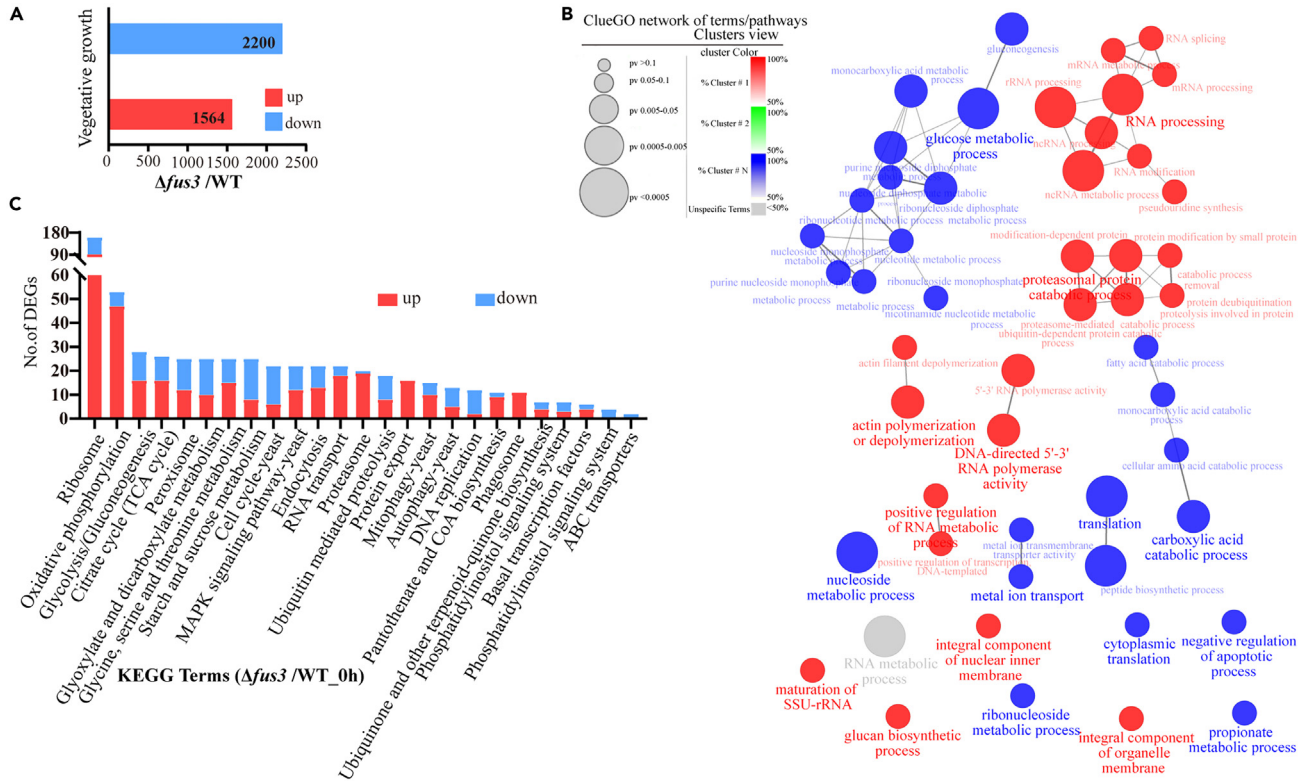

Figure 6. Comparison of transcriptional profiles in WT and Δ*fus3* mutant strains at the vegetative growth stage

(A) Numbers of differentially expressed genes (DEGs) in the Δ*fus3* mutant versus WT strain.

(B) Gene ontology (GO) enrichment of up- and downregulated DEGs, shown using Cytoscape Cluego. Red shapes indicate upregulation, and blue shapes indicate downregulation.

(C) KEGG pathway enrichment of the DEGs ($p < 0.05$) at the vegetative growth stage.

nucleoside triphosphate metabolic process, mitotic DNA integrity checkpoint signaling, DNA metabolic processes, peptide biosynthetic processes, nucleotide–sugar biosynthetic processes, and mitochondrial large ribosomal subunits and DNA strand elongation involved in DNA replication were significantly enriched at 24 hpi; and those participating in tetrahydrofolate metabolic processes, methionine metabolic processes, ammonium transmembrane transporter activity, alditol metabolic process, glucan biosynthetic process, and cellular glucan metabolic processes were enriched at 36 hpi. Furthermore, 974 co-expressed genes at three time points were involved in fatty acid biosynthetic processes, deoxyribonuclease activity, telomere maintenance, sterol metabolic processes, negative regulation of actin filament polymerization, DNA ligase (ATP) activity, carboxypeptidase activity, nitrate assimilation and gamma-aminobutyric acid metabolic process (Figure 7B). Further KEGG enrichment analysis showed that RNA transport, proteasome, peroxisome, glyoxylate, and dicarboxylate metabolism, and SNARE interactions, as well as vesicular transport pathways, were significantly enriched at 12 hpi; ribosome, oxidative phosphorylation, mismatch repair, and thiamine metabolism pathways were significantly enriched at 24 hpi; and starch and sucrose metabolism and methane metabolism pathways were significantly enriched at 36 hpi (Figure 7C).

Fus3 is involved in the regulation of secondary metabolism

The compounds in the fermentation broth of the WT and Δ*fus3* mutant strains were compared by liquid chromatography-mass spectrometry (LC-MS). Volcano plot analysis showed that the metabolites of the Δ*fus3* mutant had upregulated 2,344 compounds and downregulated 2,912 compounds compared with WT (Figure 8A). The top 20 upregulated compounds include ethyl myristate, hexadecasphinganine, 4-indolecarbaldehyde, and 2-hydroxycaproic acid (Table S8), and the top 20 downregulated compounds include delcosine, norethisterone acetate, and retosiban (Table S9). The compound peaks of the Δ*fus3* mutant were significantly different from the WT at multiple retention time points in the negative metabolic

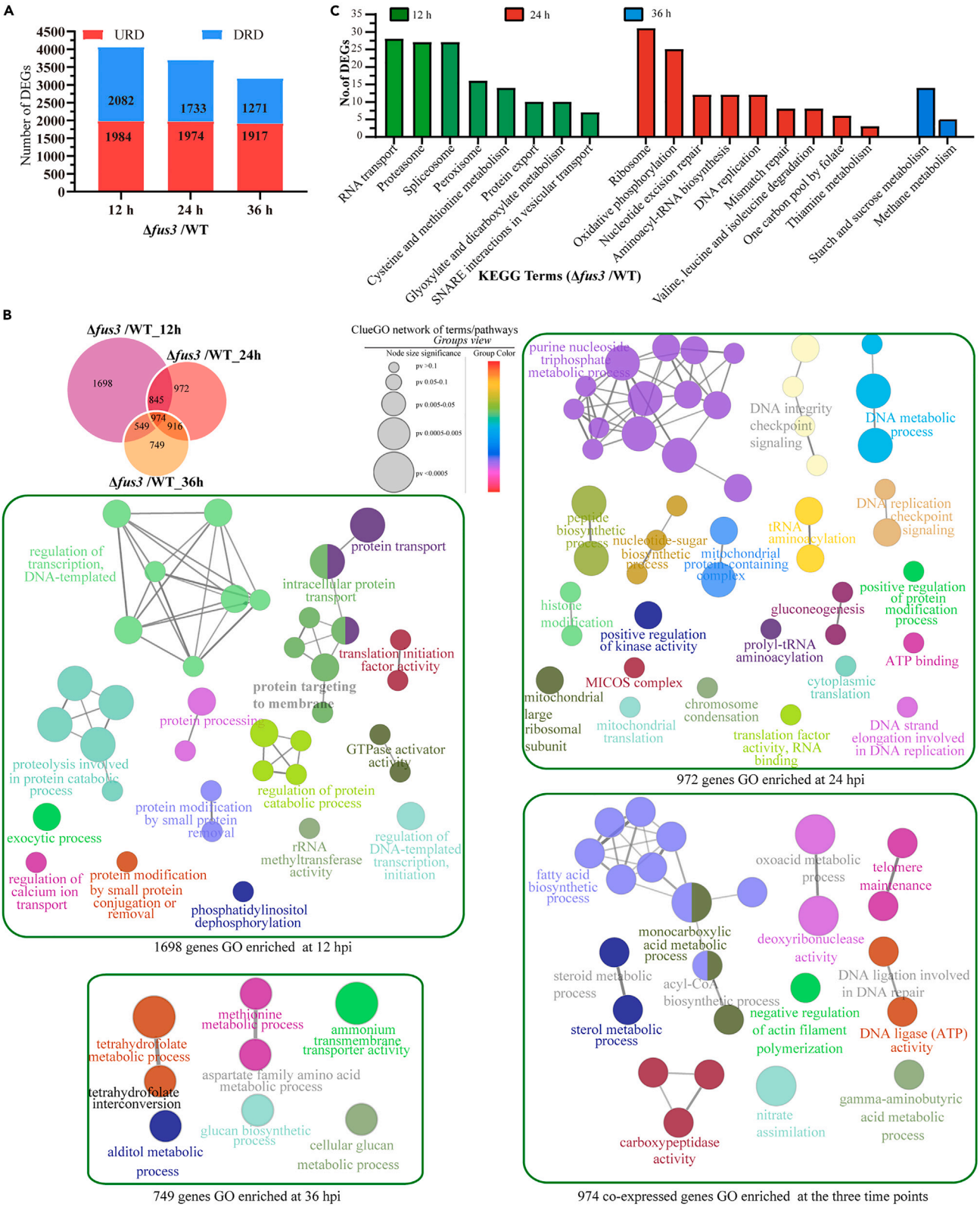
A
URD
DRD
Number of DEGs
4500
4000
3500
3000
2500
2000
1500
1000
500
0
2082
1984
1733
1974
1271
1917
12 h
24 h
36 h
Δfus3 /WT
C
12 h
24 h
36 h
No.of DEGs
35
30
25
20
15
10
5
0
RNA transport
Proteasome
Spliceosome
Peroxisome
Cysteine and methionine metabolism
Protein export
Glyoxylate and dicarboxylate metabolism
SNARE interactions in vesicular transport
Ribosome
Oxidative phosphorylation
Nucleotide excision repair
Aminoacyl-tRNA biosynthesis
DNA replication
Mismatch repair
Valine, leucine and isoleucine degradation
One carbon pool by folate
Thiamine metabolism
Starch and sucrose metabolism
Methane metabolism
KEGG Terms (Δfus3 /WT)
B
Δfus3 /WT_12h
Δfus3 /WT_24h
Δfus3 /WT_36h
1698
972
845
974
549
916
749
ClueGO network of terms/pathways
Groups view
Node size significance
Group Color
pv >0.1
pv 0.05-0.1
pv 0.005-0.05
pv 0.0005-0.005
pv <0.0005
regulation of transcription, DNA-templated
protein transport
intracellular protein transport
translation initiation factor activity
protein targeting to membrane
protein processing
GTPase activator activity
proteolysis involved in protein catabolic process
regulation of protein catabolic process
protein modification by small protein removal
exocytic process
rRNA methyltransferase activity
regulation of DNA-templated transcription, initiation
regulation of calcium ion transport
protein modification by small protein conjugation or removal
phosphatidylinositol dephosphorylation
1698 genes GO enriched at 12 hpi
purine nucleoside triphosphate metabolic process
DNA integrity checkpoint signaling
DNA metabolic process
DNA replication checkpoint signaling
peptide biosynthetic process
nucleotide-sugar biosynthetic process
tRNA aminoacylation
mitochondrial protein-containing complex
positive regulation of protein modification process
histone modification
positive regulation of kinase activity
gluconeogenesis
prolyl-tRNA aminoacylation
ATP binding
MICOS complex
cytoplasmic translation
mitochondrial large ribosomal subunit
chromosome condensation
mitochondrial translation
translation factor activity, RNA binding
DNA strand elongation involved in DNA replication
972 genes GO enriched at 24 hpi
fatty acid biosynthetic process
oxoacid metabolic process
telomere maintenance
monocarboxylic acid metabolic process
deoxyribonuclease activity
steroid metabolic process
acyl-CoA biosynthetic process
DNA ligation involved in DNA repair
sterol metabolic process
negative regulation of actin filament polymerization
DNA ligase (ATP) activity
carboxypeptidase activity
nitrate assimilation
gamma-aminobutyric acid metabolic process
974 co-expressed genes GO enriched at the three time points
tetrahydrofolate metabolic process
methionine metabolic process
ammonium transmembrane transporter activity
tetrahydrofolate interconversion
aspartate family amino acid metabolic process
alditol metabolic process
glucan biosynthetic process
cellular glucan metabolic process
749 genes GO enriched at 36 hpi

Figure 7. Comparison of transcriptional profiles of WT and Δ*fus3* strains during trap formation

(A) DEGs in the Δ*fus3* mutant compared with those in WT at 12, 24, and 36 hpi. URD, upregulated DEGs; DRD, downregulated DEGs.

(B) Gene ontology (GO) enrichment of the Δ*fus3* mutant compared with that in WT at 12, 24, and 36 hpi, shown using Cytoscape Cluego.

(C) KEGG pathway enrichment of the DEGs ($p < 0.05$) at12, 24, and 36 hpi.

profile (Figure 8B). In addition, the arthrobotrisins (diagnostic fragments ion at m/z 139, 393, and 429 under negative ion conditions) peak area was reduced in the Δ*fus3* mutant compared to the WT (Figures 8C and 8D). Correspondingly, the transcript levels of related genes in the gene cluster *AOL_s00215g* associated with biosynthesis of arthrobotrisins in the Δ*fus3* mutant were also altered from those in WT, and the transcription of these genes in the Δ*fus3* mutant was downregulated at the vegetative growth stage (0 h) (Figure 8E). KEGG analysis of the differentially expressed compounds revealed that they were enriched in pathways such as metabolic pathways and biosynthesis of secondary metabolites, microbial metabolism in diverse environments, and the biosynthesis of ubiquinone and other terpenoid–quinone (Figure S4).

Prediction and analysis of proteins interacting with Fus3

A total of 278 proteins (Fus3 and its putative targets) were analyzed using STRING[37] and then visualized using Cytoscape[38] (Table S10). Fus3 can genetic interaction with these proteins, which are involved in the MAPK signaling pathway, cell cycle, meiosis, basal transcription factors, nucleotide excision repair, DNA replication, ubiquitin mediated proteolysis, mismatch repair, homologous recombination, non-homologous end-joining, and base excision repair (Figure 9A). These genes that are involved in cell communication were then further analyzed using ClueGo in Cytoscape, and it was found that these genes were mainly involved in the response to extracellular stimuli, the regulation of signal transduction, membrane docking, the regulation of cellular processes, mitochondrial transmembrane transport, regulation of calcium ion transport, signal peptide processing, membrane fusion, and cell morphogenesis (Figure 9B). In addition, several predicted interacting proteins were further verified by Y2H, showing that Fus3 interacts with transcription factor Ste12 (AOL_s00097g514), developmental regulator FlbA (AOL_s00215g516), and protein tyrosine phosphatases Pyp1 (AOL_s00043g69) and Ptp (AOL_s00169g50) (Figure 9C).

DISCUSSION

In yeasts and several filamentous fungi, Fus3/Kss1 is an indispensable component of the MAPK signaling cascade, which has been identified to regulate sexual and asexual development, cell fusion, host infection/virulence, and/or stress response, and production of secondary metabolites.[2,3,13] In this study, we identified an orthologous Fus3 in *A. oligospora*, the sixteen selected Fus3 homologous proteins share high sequence identity, indicating that Fus3 is evolutionarily conserved in fungi. Deletion of *fus3* was found to affect mycelial growth, conidiation, and trap formation, which is similar to previous reports[32]; Furtherly, we also found that the Fus3 loss impaired the number of cell nuclei, endocytosis, stress response, hyphal fusion, DNA damage, mitochondrial morphology, autophagy, and secondary metabolism.

The disruption of *fus3* caused severe defects with respect to hyphal development, including slowed radial growth and a decrease in the number of aerial hyphae, which was similar to what was observed in the Δ*fus3* mutant of the *Trichoderma brevicrassum*.[39] However, the Δ*fus3* mutant of *A. flavus*,[13] *A. oryzae*,[40] and *B. cinerea*[6] only displayed slower growth and exhibited no changes in number of aerial hyphae. Meanwhile, our results differed from those obtained for the Δ*fus3* mutants (Δ*pmk1*) in *M. grisea*[8] and *Metarhizium robertsii*,[41] in which Fus3 is nonessential for vegetative growth. In addition, in this study, the hyphal septum of the Δ*fus3* mutant increased compared with WT, and some hyphae were inflated. Furthermore, transcriptome analysis revealed that the expression of genes involved in glycolysis/gluconeogenesis, citrate cycle, and glyoxylate and dicarboxylate metabolism was altered in the Δ*fus3* mutant. These findings indicate that Fus3 is critical for vegetative growth; however, its functional activity may vary among fungal species.

The main way for filamentous fungi to reproduce is to produce conidia, and the ability to produce conidia is one of the key factors determining the fecundity and fitness of filamentous fungi.[42] The conidiophore of *A. oligospora* consists of one to six nodules, and conidia are densely attached to denticles with nodular protrusions.[43] In this study, deletion of *fus3* resulted in only 1–2 spores being attached on the conidiophore, and spore yield was significantly reduced, with similar results having been reported in other fungal species. For example, the conidial yield of the Δ*fus3* mutant in *A. flavus* was significantly reduced; in addition, the conidia head and conidiophore were maldeveloped and sterile, the sclerotia yield of the Δ*fus3* was severely decreased compared with the WT.[13] The Δ*fus3* of *A. oryzae* exhibited severe conidiation defects, and did

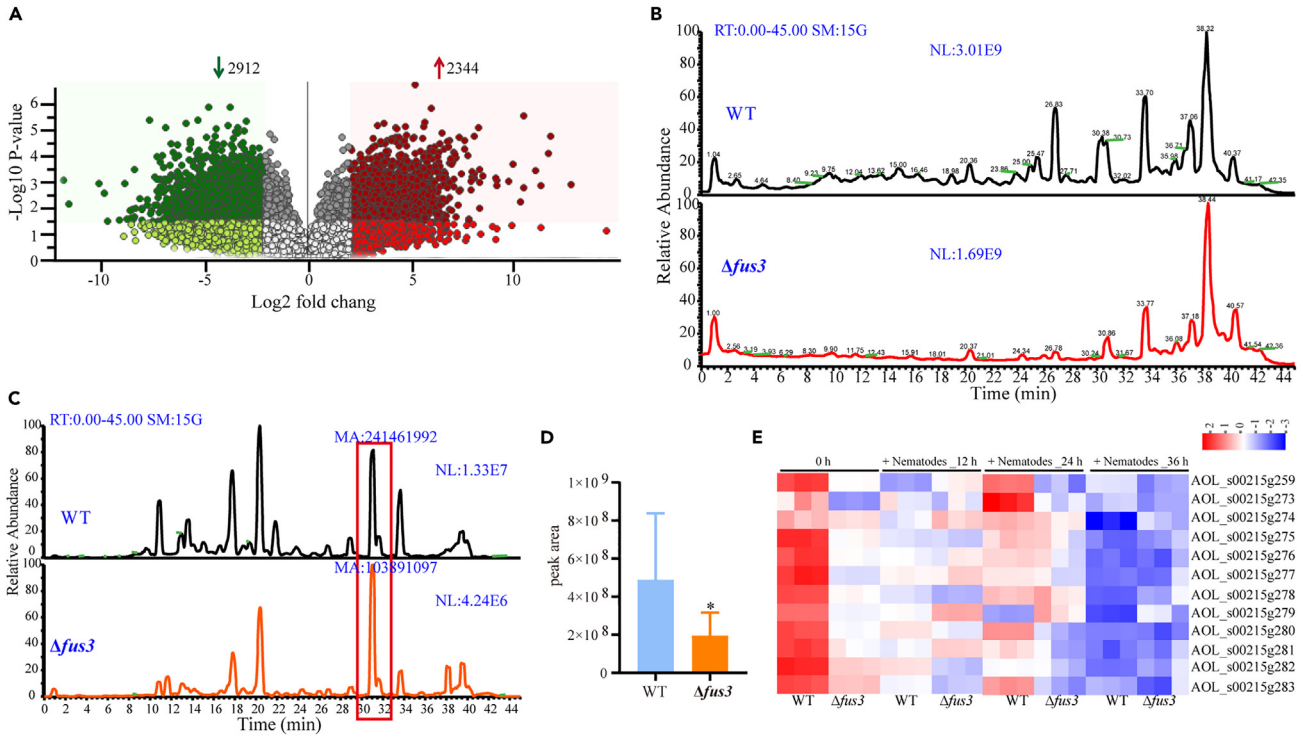

Figure 8. LC-MS analysis of WT and Δ*fus3* strains

(A) Volcanic map of metabolites differentially produced by WT and Δ*fus3* strains.

(B) HPLC profiling of WT and Δ*fus3* strains.

(C) Negative ion metabolic profiles of WT and Δ*fus3* strains; the red box indicates the peak area of arthrobotrisins.

(D) Analysis of peak area of arthrobotrisins. (the data are presented as the mean ± SD from three independent experiments, *$p < 0.05$).

(E) Transcription heatmap of gene cluster *AOL_s00215g* associated with arthrobotrisin biosynthesis.

not form any sclerotia.[40] The conidial yield of the Δ*fus3* mutant in *M. robertsii* was significantly reduced.[41] However, our results differ from those obtained for the Δ*fus3* mutant (Δ*tbmk*) in the *T. brevicrassum*, which did not change conidiation.[39] These findings indicate that Fus3 play a critical role in sporulation and morphological development of conidiophores in *A. oligospora* and most filamentous fungi.

Fungi can respond rapidly to external environmental stimuli or stress, and regulate a series of cellular activities of cells to adapt to environmental changes.[44] In this study, under hypertonic stress, the growth of the Δ*fus3* mutant was inhibited; these changes are similar to those of the Δ*fus3* mutant in *M. robertsii*,[41] whereas the Δ*tbmk* mutant of the *T. breve* showed no significant response to high osmolarity conditions caused by 0.5 M NaCl.[39] Under oxidative stress, the growth of the Δ*fus3* mutant was remarkably inhibited, with these changes being similar to those in the Δ*fus3* mutant (Δ*tbmk*) in the *T. breve* under oxidative stress.[39] Meanwhile, no significant differences in growth rate with respect to stress of 0.01% H_2O_2 were observed between the Δ*fus3* mutant and *M. robertsii* WT strain.[41] At the same time, the expression levels of genes *glt*, *cat1*, and *glr* were significantly changed in Δ*fus3* mutant compared with WT. In addition, the growth of the Δ*fus3* mutant was inhibited under cell wall-perturbing stress, and these changes were similar to the increased sensitivity of the Δ*fus3* mutant to Congo red in *T. breve*.[39] In *M. robertsii*, the Δ*fus3* mutant was significantly inhibited on PDA plates containing Congo red.[41] Correspondingly, the transcripts of several genes related to cell wall biosynthesis were significantly altered in the Δ*fus3* mutant. Overall, these results indicate that Fus3 is important for environmental adaptation in *A. oligospora* and most of fungi.

Communication and cell fusion occurring between hyphae in colonies are important for strengthening the colony structure and supporting the development of complex structures such as aerial hyphae and sexual reproduction structures.[3] In this study, the deletion of *fus3* resulted in defects in hyphal cell fusion consistent with those reported in previous studies on the involvement of Fus3 in cell fusion in fungi. The Fus3 orthologs were shown to be essential for cell fusion in *S. cerevisiae*,[4] *N. crassa*,[5] *A. nidulans*,[45] and *A. oryzae*.[40]

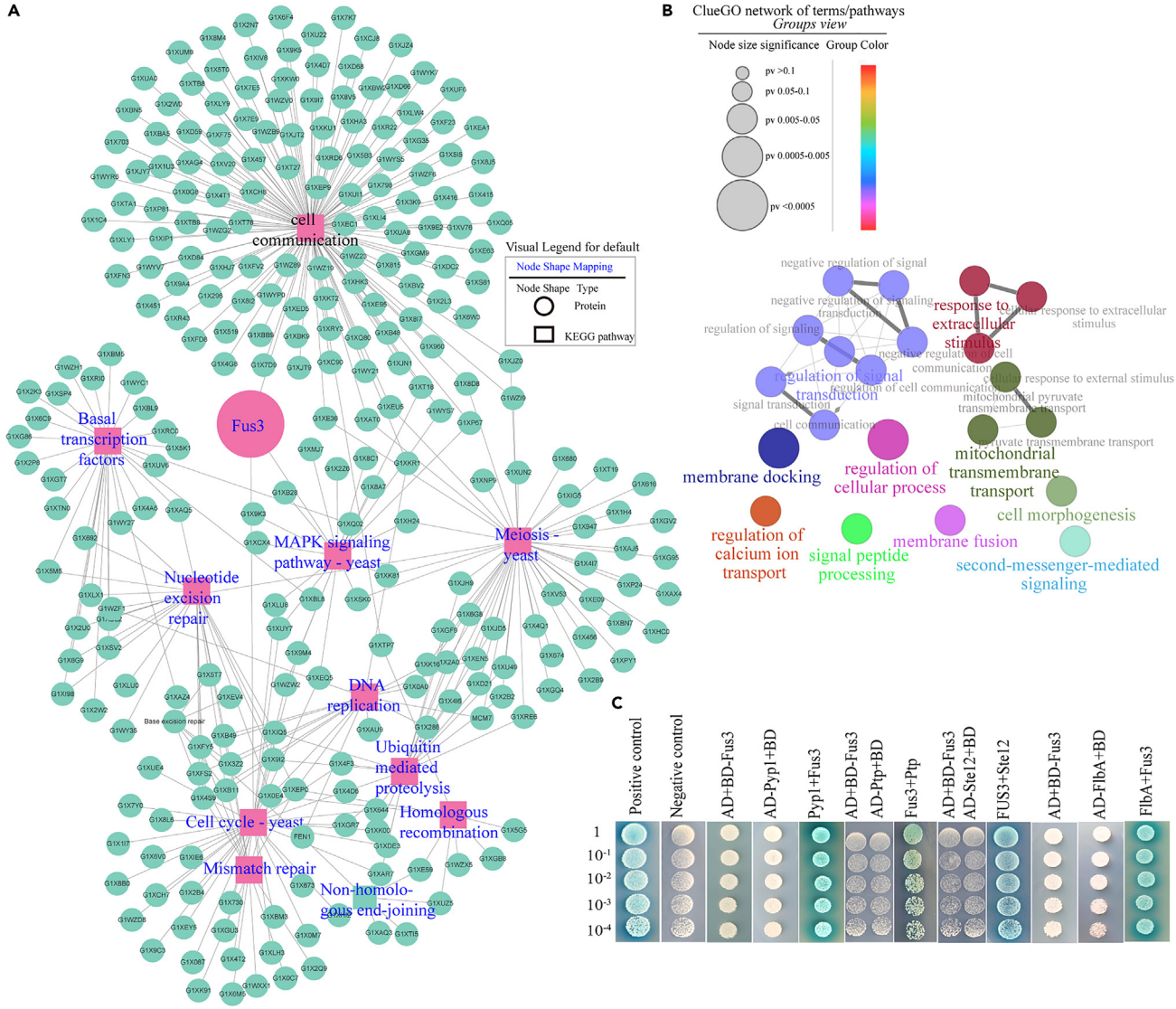

Figure 9. Analyses of regulatory network and target genes of Fus3

(A) Interconnected gene regulatory networks of Fus3.

(B) GO enrichment associated with cellular communication, shown using Cytoscape Cluego.

(C) Analysis of protein interactions using yeast two-hybrid screening with β-D-galactosidase.

In *N. crassa*, the Fus3 ortholog (MAK-2) is essential for germling and hyphal fusion, which normally takes place during germination and colony development.[5] Importantly, hyphal cell fusion plays a specific role in trap formation in NT fungi, as in the NT fungus *Duddingtonia flagrans*, deletion of *sofT* (hyphal anastomosis gene) resulted in defects in the ring closure of traps due to the anastomoses present in normal vegetative hyphae being completely inhibited.[46] Similarly, deletion of *fus3* resulted in defects in trap cell fusion, such that the Δ*fus3* mutant was not able to produce typical three-dimensional networks to capture nematodes, and could only form spiral hyphal coils. In addition, WBs were unable to seal the damaged septal pores, and the number of ED bodies in the trap cells of the Δ*fus3* mutant was reduced. ED bodies are unique structures in the trap cells of NT fungi, and are organelles associated with peroxisomes that provide energy for invading hyphae.[47,48] WBs are peroxisome-derived dense-core vesicles unique to several filamentous ascomycetes, and have been shown to be involved in regulating trap formation in *A. oligospora*.[49] Recently, two peroxisome biogenesis genes, *Aopex1* and *Aopex6*, were identified in *A. oligospora*, absence of *Aopex1* and *Aopex6* resulted in a failure to produce traps and conidia.[50] In addition, transcriptome analysis found that the absence of *fus3* resulted in changes in processes associated with

cell communication, membrane fusion, and regulation of calcium ion transport. Moreover, the nematode predatory efficiency was significantly reduced due to the inability of the Δ*fus3* mutant to produce typical traps. Similarly, the Δ*ku70 fus3* mutant of *A. oligospora* (strain TWF154) completely lost the ability to produce traps,[32] and the Δ*pmk1* mutant (an *fus3* homolog) of the rice blast fungus *M. grisea* failed to complete the formation of mature appressoria and failed to grow invasively in rice plants.[8] In addition, these effects are consistent with those caused by *fus3* mutations in *M. robertsii*,[41] *C. heterostrophus*,[11] *Botrytis cinerea*.[6] These results suggest that Fus3 plays an important role in cell communication and hyphal fusion in *A. oligospora* and other fungi, and Fus3 plays a conserved and indispensable role in fungal pathogenesis.

In recent years, comparative transcriptome analysis has been broadly used to reveal the gene expression changes between fungi and their hosts.[13,51–54] In this study, the absence of *fus3* resulted in several genes that are involved in regulation of multiple cellular processes being altered at the transcriptional level, suggesting that Fus3 is a multifunctional regulator involved in key cellular processes during vegetative growth and trap formation. In transcriptome analysis, mitotic cell cycle process, autophagy, and mitophagy were found to be associated with hyphal growth, sporulation, and the DNA repair process. DNA repair is an important biological process that maintains genome stability and protects DNA from damage and mutation, including mismatch, base excision, and nucleotide excision repair.[55] In our results, the partial hyphal cells of the Δ*fus3* mutant were enlarged and deformed, and the hyphae and spores of the Δ*fus3* mutant exhibited considerable DNA damage. Furthermore, mitophagy is an autophagic process that selectively sequesters and degrades damaged or incomplete mitochondria, and is involved in maintaining the integrity of mitochondrial network function and cellular homeostasis.[56] Consistently, in this study, the transcriptome revealed that an integral component of the organelle membrane changed after *fus3* disruption, phenotypic analysis revealed that mitochondrial membranes of the Δ*fus3* mutant exhibited considerable damage, and we also observed mitophagy in Δ*fus3* mutant cells. In addition, transcriptome analysis also revealed changes in cell fusion, consistent with the failure of the Δ*fus3* mutant hyphal cells to fuse in our phenotypic experiments. Similarly, transcriptome analysis showed that endocytosis and the exocytic process were significantly enriched. Correspondingly, FM4-64 staining and TEM observation showed that the Δ*fus3* mutant exhibited an altered endocytosis process and endocytosis structures compared with WT.

A regulatory network of Fus3 was constructed on the basis of phenotypic and transcriptome analysis, and further Y2H validation found that AoSte12, AoFlbA, AoPyp1, and AoPtp are potential targets of Fus3. Among them, transcription factor Ste12 has been reported to be the downstream target of Fus3 in several fungi, such as *S. cerevisiae*, *N. crassa*,[57] *M. grisea*,[58] and *A. flavus*.[13] FlbA encodes a G protein signaling regulator (RGS) domain protein, which negatively regulates vegetative growth.[59] In our recent work, deletion of *AoflbA* resulted in a severe defect in the conidiation and trap formation of *A. oligospora*.[60] In addition, Ptp and Pyp1 are involved in cell signal transduction, regulating cell growth, differentiation, metabolism, gene transcription and other processes.[61] In fission yeast, Pyp1 act as negative regulators of mitosis, controlling cell size at division and negatively regulating nutrient monitoring pathways.[62] Therefore, Fus3 can interact with diverse transcription factors and regulators, thus regulating multiple cellular and biological processes in *A. oligospora*.

It has been shown that Fus3 orthologs are involved in the secondary metabolism of several filamentous fungi, such as *A. fumigatus*,[12] *A. flavus*,[13,14] and *T. brevicrassum*.[39] In this study, the metabolites of the Δ*fus3* mutant were significantly altered compared with WT. In addition, the content of arthrobotrisins in the Δ*fus3* mutant, a special group of metabolites identified in *A. oligospora* and other NT fungi, was found to be reduced by means of metabolome analysis, and the expressional levels of gene cluster *AOL_s00215g* associated with biosynthesis of arthrobotrisins were also downregulated during vegetative growth. Arthrobotrisins produced by *A. oligospora* and other NT fungi are involved in the regulation of hyphal growth and trap formation.[63,64] These results suggest that Fus3 plays an important regulatory role in secondary metabolism in diverse fungi.

In summary, our results show that Fus3 is an essential component of the MAPK signaling cascade, is indispensable for hyphal fusion, trap morphogenesis, and pathogenicity, and plays an important role in asexual growth and development, conidiation, stress response, DNA damage, autophagy, and secondary metabolism. In addition, the regulatory network analysis of Fus3 suggested that it can impair diverse phenotypic traits by regulating downstream target genes that are involved in protein synthesis and processing, autophagy, oxidative phosphorylation, cell cycle, endocytosis, peroxisome, and proteasome. In summary, our

study revealed the conserved roles of Fus3 in different fungi, such as mycelial growth, sexual development, and autolysis, importantly, several unique effects of Fus3 were found in this study including the hyphal fusion, trap morphogenesis, and nematode predation. Our study provides deep insights into the mechanism of MAPK signaling in trap formation and lifestyle transition in NT fungi, and lays a foundation for uncovering the regulatory mechanism of NT fungal cell fusion, asexual reproduction, and pathogenicity.

Limitations of the study

In this study, we constructed the regulatory networks of Fus3 based on the transcriptomic data and STRING analysis. Our results showed that Fus3 can interact with numerous proteins, which are involved in the MAPK signaling pathway and multiple cellular processes, whereas we did not confirm what kind of interaction between them? In addition, several predicted interacting proteins were verified by Y2H, showing that Fus3 interacts with several targets including Ste12, FlbA, Pyp1, and Ptp, however the interaction between Fus3 and targets should be furtherly confirmed by other methods, such as co-immunoprecipitation and pull-down assays.

STAR★METHODS

Detailed methods are provided in the online version of this paper and include the following:

- KEY RESOURCES TABLE
- RESOURCE AVAILABILITY
  - Lead contact
  - Materials availability
  - Data and code availability
- EXPERIMENTAL MODEL AND STUDY PARTICIPANT DETAILS
  - Fungal strains
  - Bacterial strain
  - Nematode
- METHOD DETAILS
  - Sequence analysis of Fus3
  - Deletion of fus3
  - Analysis of vegetative growth, morphogenesis, and conidiation
  - Stress assays
  - Trap formation and morphogenesis
  - Transcriptome sequencing and analysis
  - LC-MS assay
  - RT-qPCR analysis
  - Y2H screening
  - Analysis of regulatory network of Fus3
- QUANTIFICATION AND STATISTICAL ANALYSIS

SUPPLEMENTAL INFORMATION

Supplemental information can be found online at https://doi.org/10.1016/j.isci.2023.107404.

ACKNOWLEDGMENTS

We are grateful to Microbial Library of the Germplasm Bank of Wild Species from Southwest China for preserving and providing experimental strains, and Guo Ying-qi (Kunming Institute of Zoology, Chinese Academy of Sciences) for her help with taking and analyzing TEM images. Funding for this study was provided by National Natural Science Foundation of China (nos. 31960556, 32160665, and U1402265), Special fund of the Yunnan University "double first-class" construction, Yunnan Fundamental Research Projects (nos. 202201BC070004 and 202001BB050004), and General Project of Yunnan Provincial Department of Science and Technology (202101AT070779).

AUTHOR CONTRIBUTIONS

K-Q.Z. and J.Y. conceived and designed the study. M.X. and N.B. performed the experiments. M.X., N.B., X.Y., and Y.L. analyzed the data. M.X. prepared figures and tables. M.X. and J.Y. contributed to manuscript preparation and revision. All authors read and approved the final manuscript.

DECLARATION OF INTERESTS

We declare that we have no conflicts of interests.

Received: November 26, 2022
Revised: April 7, 2023
Accepted: July 12, 2023
Published: August 7, 2023

REFERENCES

1. Xu, J.R. (2000). Map kinases in fungal pathogens. Fungal Genet. Biol. *31*, 137–152.

2. Jiang, C., Zhang, X., Liu, H., and Xu, J.R. (2018). Mitogen-activated protein kinase signaling in plant pathogenic fungi. PLoS Pathog. *14*, e1006875.

3. Fischer, M.S., and Glass, N.L. (2019). Communicate and fuse: How filamentous fungi establish and maintain an interconnected mycelial network. Front. Microbiol. *10*, 619.

4. Fujimura, H.A. (1994). Yeast homolog of mammalian mitogen-activated protein kinase, FUS3/DAC2 kinase, is required both for cell fusion and for G1 arrest of the cell cycle and morphological changes by the cdc37 mutation. J. Cell Sci. *107*, 2617–2622.

5. Herzog, S., Schumann, M.R., and Fleißner, A. (2015). Cell fusion in *Neurospora crassa*. Curr. Opin. Microbiol. *28*, 53–59.

6. Zheng, L., Campbell, M., Murphy, J., Lam, S., and Xu, J.R. (2000). The *BMP1* gene is essential for pathogenicity in the gray mold fungus *Botrytis cinerea*. Mol. Plant Microbe Interact. *13*, 724–732.

7. Turrà, D., Segorbe, D., and Di Pietro, A. (2014). Protein kinases in plant-pathogenic fungi: Conserved regulators of infection. Annu. Rev. Phytopathol. *52*, 267–288.

8. Xu, J.R., and Hamer, J.E. (1996). MAP kinase and cAMP signaling regulate infection structure formation and pathogenic growth in the rice blast fungus *Magnaporthe grisea*. Genes Dev. *10*, 2696–2706.

9. Kang, J.Y., Chun, J., Jun, S.C., Han, D.M., Chae, K.S., and Jahng, K.Y. (2013). The MpkB MAP kinase plays a role in autolysis and conidiation of *Aspergillus nidulans*. Fungal Genet. Biol. *61*, 42–49.

10. Ruiz-Roldán, M.C., Maier, F.J., and Schäfer, W. (2001). PTK1, a mitogen-activated-protein kinase gene, is required for conidiation, appressorium formation, and pathogenicity of *Pyrenophora teres* on barley. Mol. Plant Microbe Interact. *14*, 116–125.

11. Lev, S., Sharon, A., Hadar, R., Ma, H., and Horwitz, B.A. (1999). A mitogen-activated protein kinase of the corn leaf pathogen *Cochliobolus heterostrophus* is involved in conidiation, appressorium formation, and pathogenicity: diverse roles for mitogen-activated protein kinase homologs in foliar pathogens. Proc. Natl. Acad. Sci. USA *96*, 13542–13547.

12. Jain, R., Valiante, V., Remme, N., Docimo, T., Heinekamp, T., Hertweck, C., Gershenzon, J., Haas, H., and Brakhage, A.A. (2011). The MAP kinase MpkA controls cell wall integrity, oxidative stress response, gliotoxin production and iron adaptation in *Aspergillus fumigatus*. Mol. Microbiol. *82*, 39–53.

13. Ma, L., Li, X., Xing, F., Ma, J., Ma, X., and Jiang, Y. (2022). Fus3, as a critical kinase in MAPK cascade, regulates aflatoxin biosynthesis by controlling the substrate supply in *Aspergillus flavus*, rather than the cluster genes modulation. Microbiol. Spectr. *10*, e0126921.

14. Frawley, D., Greco, C., Oakley, B., Alhussain, M.M., Fleming, A.B., Keller, N.P., and Bayram, Ö. (2020). The tetrameric pheromone module SteC-MkkB-MpkB SteD regulates asexual sporulation, sclerotia formation and aflatoxin production in *Aspergillus flavus*. Cell Microbiol. *22*, e13192.

15. Frawley, D., and Bayram, Ö. (2020). The pheromone response module, a mitogen-activated protein kinase pathway implicated in the regulation of fungal development, secondary metabolism and pathogenicity. Fungal Genet. Biol. *144*, 103469.

16. Bayram, Ö., Bayram, Ö.S., Ahmed, Y.L., Maruyama, J.I., Valerius, O., Rizzoli, S.O., Ficner, R., Irniger, S., and Braus, G.H. (2012). The *Aspergillus nidulans* MAPK module AnSte11-Ste50-Ste7-Fus3 controls development and secondary metabolism. PLoS Genet. *8*, e1002816.

17. Atoui, A., Bao, D., Kaur, N., Grayburn, W.S., and Calvo, A.M. (2008). *Aspergillus nidulans* natural product biosynthesis is regulated by mpkB, a putative pheromone response mitogen-activated protein kinase. Appl. Environ. Microbiol. *74*, 3596–3600.

18. Zhu, M.C., Li, X.M., Zhao, N., Yang, L., Zhang, K.Q., and Yang, J.K. (2022). Regulatory mechanism of trap formation in the nematode-trapping fungi. J. Fungi *8*, 406.

19. Ji, X., Yu, Z., Yang, J., Xu, J., Zhang, Y., Liu, S., Zou, C., Li, J., Liang, L., and Zhang, K.Q. (2020). Expansion of adhesion genes drives pathogenic adaptation of nematode-trapping fungi. iScience *23*, 101057.

20. Xie, M., Wang, Y., Tang, L., Yang, L., Zhou, D., Li, Q., Niu, X., Zhang, K.Q., and Yang, J. (2019). AoStuA, an APSES transcription factor, regulates the conidiation, trap formation, stress resistance and pathogenicity of the nematode-trapping fungus *Arthrobotrys oligospora*. Environ. Microbiol. *21*, 4648–4661.

21. Nordbring-Hertz, B. (2004). Morphogenesis in the nematode-trapping fungus *Arthrobotrys oligospora* - an extensive plasticity of infection structures. Mycologist *18*, 125–133.

22. Bai, N., Xie, M., Liu, Q., Wang, W., Liu, Y., and Yang, J. (2023). AoSte12 is required for mycelial development, conidiation, trap morphogenesis, and secondary metabolism by regulating hyphal fusion in nematode-trapping fungus *Arthrobotrys oligospora*. Microbiol. Spectr. *11*, e0395722.

23. Yang, J., Wang, L., Ji, X., Feng, Y., Li, X., Zou, C., Xu, J., Ren, Y., Mi, Q., Wu, J., et al. (2011). Genomic and proteomic analyses of the fungus *Arthrobotrys oligospora* provide insights into nematode-trap formation. PLoS Pathog. *7*, e1002179.

24. Yang, C.T., Vidal-Diez de Ulzurrun, G., Gonçalves, A.P., Lin, H.C., Chang, C.W., Huang, T.Y., Chen, S.A., Lai, C.K., Tsai, I.J., Schroeder, F.C., et al. (2020). Natural diversity in the predatory behavior facilitates the establishment of a robust model strain for nematode-trapping fungi. Proc. Natl. Acad. Sci. USA *117*, 6762–6770.

25. Bai, N., Zhang, G., Wang, W., Feng, H., Yang, X., Zheng, Y., Yang, L., Xie, M., Zhang, K.Q., and Yang, J. (2022). Ric8 acts as a regulator of G-protein signalling required for nematode-trapping lifecycle of *Arthrobotrys oligospora*. Environ. Microbiol. *24*, 1714–1730.

26. Yang, L., Li, X., Xie, M., Bai, N., Yang, J., Jiang, K., Zhang, K.Q., and Yang, J. (2021). Pleiotropic roles of Ras GTPases in the nematode-trapping fungus *Arthrobotrys oligospora* identified through multi-omics analyses. iScience *24*, 102820.

27. Yang, L., Li, X., Bai, N., Yang, X., Zhang, K.Q., and Yang, J. (2022). Transcriptomic analysis reveals that Rho GTPases regulate trap development and lifestyle transition of the nematode-trapping fungus *Arthrobotrys oligospora*. Microbiol. Spectr. *10*, e0175921.

28. Zhu, M.C., Zhao, N., Liu, Y.K., Li, X.M., Zhen, Z.Y., Zheng, Y.Q., Zhang, K.Q., and Yang, J.K. (2022). The cAMP-PKA signalling pathway regulates hyphal growth, conidiation, trap morphogenesis, stress tolerance, and autophagy in *Arthrobotrys oligospora*. Environ. Microbiol. *24*, 6524–6538.

29. Kuo, C.Y., Chen, S.A., and Hsueh, Y.P. (2020). The high osmolarity glycerol (HOG) pathway functions in osmosensing, trap morphogenesis and conidiation of the nematode-trapping fungus *Arthrobotrys oligospora*. J. Fungi *6*, 191.

30. Xie, M., Yang, J., Jiang, K., Bai, N., Zhu, M., Zhu, Y., Zhang, K.Q., and Yang, J. (2021). AoBck1 and AoMkk1 are necessary to maintain cell wall integrity, vegetative growth, conidiation, stress resistance, and pathogenicity in the nematode-trapping fungus *Arthrobotrys oligospora*. Front. Microbiol. *12*, 649582.

31. Zhen, Z., Xing, X., Xie, M., Yang, L., Yang, X., Zheng, Y., Chen, Y., Ma, N., Li, Q., Zhang, K.Q., and Yang, J. (2018). MAP kinase Slt2 orthologs play similar roles in conidiation, trap formation, and pathogenicity in two nematode-trapping fungi. Fungal Genet. Biol. *116*, 42–50.

32. Chen, S.A., Lin, H.C., Schroeder, F.C., and Hsueh, Y.P. (2021). Prey sensing and response in a nematode-trapping fungus is governed by the MAPK pheromone response pathway. Genetics *217*, iyaa008.

33. Adams, T.H., Wieser, J.K., and Yu, J.H. (1998). Asexual sporulation in *Aspergillus nidulans*. Microbiol. Mol. Biol. Rev. *62*, 35–54.

34. Liu, J., Wang, Z.K., Sun, H.H., Ying, S.H., and Feng, M.G. (2017). Characterization of the Hog1 MAPK pathway in the entomopathogenic fungus *Beauveria bassiana*. Environ. Microbiol. *19*, 1808–1821.

35. Fleissner, A., Sarkar, S., Jacobson, D.J., Roca, M.G., Read, N.D., and Glass, N.L. (2005). The so locus is required for vegetative cell fusion and postfertilization events in *Neurospora crassa*. Eukaryot. Cell *4*, 920–930.

36. Meisinger, C., Rissler, M., Chacinska, A., Szklarz, L.K.S., Milenkovic, D., Kozjak, V., Schönfisch, B., Lohaus, C., Meyer, H.E., Yaffe, M.P., et al. (2004). The mitochondrial morphology protein Mdm10 functions in assembly of the preprotein translocase of the outer membrane. Dev. Cell *7*, 61–71.

37. Hao, S., Li, S., Wang, J., Zhao, L., Yan, Y., Cao, Q., Wu, T., Liu, L., and Wang, C. (2018). Transcriptome analysis of phycocyanin-mediated inhibitory functions on non-small cell lung cancer A549 cell growth. Mar. Drugs *16*, 511.

38. Franz, M., Lopes, C.T., Huck, G., Dong, Y., Sumer, O., and Bader, G.D. (2016). Cytoscape.js: a graph theory library for visualisation and analysis. Bioinformatics *32*, 309–311.

39. Zhang, Y., and Zhuang, W.Y. (2022). MAPK cascades mediating biocontrol activity of *Trichoderma brevicrassum* strain TC967. J. Agric. Food Chem. *70*, 2762–2775.

40. Katayama, T., Bayram, Ö., Mo, T., Karahoda, B., Valerius, O., Takemoto, D., Braus, G.H., Kitamoto, K., and Maruyama, J.I. (2021). Novel Fus3- and Ste12-interacting protein FsiA activates cell fusion-related genes in both Ste12-dependent and -independent manners in Ascomycete filamentous fungi. Mol. Microbiol. *115*, 723–738.

41. Chen, X., Xu, C., Qian, Y., Liu, R., Zhang, Q., Zeng, G., Zhang, X., Zhao, H., and Fang, W. (2016). MAPK cascade-mediated regulation of pathogenicity, conidiation and tolerance to abiotic stresses in the entomopathogenic fungus *Metarhizium robertsii*. Environ. Microbiol. *18*, 1048–1062.

42. Zhang, G., Zheng, Y., Ma, Y., Yang, L., Xie, M., Zhou, D., Niu, X., Zhang, K.Q., and Yang, J. (2019). The velvet proteins VosA and VelB play different roles in conidiation, trap formation, and pathogenicity in the nematode-trapping fungus *Arthrobotrys oligospora*. Front. Microbiol. *10*, 1917.

43. Yu, Z., Mo, M., Zhang, Y., and Zhang, K.Q. (2014). Taxonomy of nematode-trapping fungi from orbiliaceae, ascomycota. In Nematode-Trapping Fungi. Fungal Diversity Research Series, K.Q. Zhang and K. Hyde, eds. (Springer), pp. 41–210.

44. Hamel, L.P., Nicole, M.C., Duplessis, S., and Ellis, B.E. (2012). Mitogen-activated protein kinase signaling in plant-interacting fungi: Distinct messages from conserved messengers. Plant Cell *24*, 1327–1351.

45. Jun, S.C., Lee, S.J., Park, H.J., Kang, J.Y., Leem, Y.E., Yang, T.H., Chang, M.H., Kim, J.M., Jang, S.H., Kim, H.G., et al. (2011). The MpkB MAP kinase plays a role in post-karyogamy processes as well as in hyphal anastomosis during sexual development in *Aspergillus nidulans*. J. Microbiol. *49*, 418–430.

46. Youssar, L., Wernet, V., Hensel, N., Yu, X., Hildebrand, H.G., Schreckenberger, B., Kriegler, M., Hetzer, B., Frankino, P., Dillin, A., and Fischer, R. (2019). Intercellular communication is required for trap formation in the nematode-trapping fungus *Duddingtonia flagrans*. PLoS Genet. *15*, e1008029.

47. Veenhuis, M., Nordbring-Hertz, B., and Harder, W. (1985). Development of fate of electron-dense microbodies in trap cells of the nematophagous fungus *Arthrobotrys oligospora*. Antonie Van Leeuwenhoek *51*, 399–407.

48. Liu, Q., Li, D., Bai, N., Zhu, Y., and Yang, J. (2023). Peroxin Pex14/17 is required for trap formation, and plays pleiotropic roles in mycelial development, stress response, and secondary metabolism in *Arthrobotrys oligospora*. mSphere *8*, e0001223.

49. Liang, L., Gao, H., Li, J., Liu, L., Liu, Z., and Zhang, K.Q. (2017). The Woronin body in the nematophagous fungus *Arthrobotrys oligospora* is essential for trap formation and efficient pathogenesis. Fungal Biol. *121*, 11–20.

50. Liu, Q., Li, D., Jiang, K., Zhang, K.Q., and Yang, J. (2022). *AoPEX1* and *AoPEX6* are required for mycelial growth, conidiation, stress response, fatty acid utilization, and trap formation in *Arthrobotrys oligospora*. Microbiol. Spectr. *10*, e0027522.

51. Xie, M., Ma, N., Bai, N., Yang, L., Yang, X., Zhang, K.Q., and Yang, J. (2022). PKC-SWI6 signaling regulates asexual development, cell wall integrity, stress response, and lifestyle transition in the nematode-trapping fungus *Arthrobotrys oligospora*. Sci. China Life Sci. *65*, 2455–2471.

52. Yang, J., Wang, W., Liu, Y., Xie, M., and Yang, J. (2023). The MADS-box transcription factor AoRlmA is involved in the regulation of mycelium development, conidiation, cell-wall integrity, stress response, and trap formation of *Arthrobotrys oligospora*. Microbiol. Res. *268*, 127299.

53. Hou, J., Zhang, H., Ding, J.L., Feng, M.G., and Ying, S.H. (2023). Transcriptomic investigation reveals a physiological mechanism for *Beauveria bassiana* to survive under linoleic acid stress. iScience *26*, 106551.

54. Wang, W., Zhao, Y., Bai, N., Zhang, K.Q., and Yang, J. (2022). AMPK is involved in regulating the utilization of carbon sources, conidiation, pathogenicity, and stress response of the nematode-trapping fungus *Arthrobotrys oligospora*. Microbiol. Spectr. *10*, e0222522.

55. Harper, J.W., and Elledge, S.J. (2007). The DNA damage response: ten years after. Mol. Cell *28*, 739–745.

56. Youle, R.J., and Narendra, D.P. (2011). Mechanisms of mitophagy. Nat. Rev. Mol. Cell Biol. *12*, 9–14.

57. Li, D., Bobrowicz, P., Wilkinson, H.H., and Ebbole, D.J. (2005). A mitogen-activated protein kinase pathway essential for mating and contributing to vegetative growth in *Neurospora crassa*. Genetics *170*, 1091–1104.

58. Park, G., Bruno, K.S., Staiger, C.J., Talbot, N.J., and Xu, J.R. (2004). Independent genetic mechanisms mediate turgor generation and penetration peg formation during plant infection in the rice blast fungus. Mol. Microbiol. *53*, 1695–1707.

59. D'Souza, C.A., Lee, B.N., and Adams, T.H. (2001). Characterization of the role of the FluG protein in asexual development of *Aspergillus nidulans*. Genetics *158*, 1027–1036.

60. Ma, N., Zhao, Y., Wang, Y., Yang, L., Li, D., Yang, J., Jiang, K., Zhang, K.Q., and Yang, J. (2021). Functional analysis of seven regulators of G protein signaling (RGSs) in the nematode-trapping fungus *Arthrobotrys oligospora*. Virulence *12*, 1825–1840.

61. Sun, H., and Tonks, N.K. (1994). The coordinated action of protein tyrosine phosphatases and kinases in cell signaling. Trends Biochem. Sci. *19*, 480–485.

62. Santo, P.D., Blanchard, B., and Hoffman, C.S. (1996). The *Schizosaccharomyces pombe* pyp1 protein tyrosine phosphatase negatively regulates nutrient monitoring pathways. J. Cell Sci. *109*, 1919–1925.

63. Yu, X., Hu, X., Pop, M., Wernet, N., Kirschhöfer, F., Brenner-Weiß, G., Keller, J., Bunzel, M., and Fischer, R. (2021). Fatal attraction of *Caenorhabditis elegans* to predatory fungi through 6-methyl-salicylic acid. Nat. Commun. *12*, 5462.

64. Wei, L.X., Zhang, H.X., Tan, J.L., Chu, Y.S., Li, N., Xue, H.X., Wang, Y.L., Niu, X.M., Zhang, Y., and Zhang, K.Q. (2011). Arthrobotrisins A-C, oligosporons from the nematode-trapping fungus *Arthrobotrys oligospora*. J. Nat. Prod. *74*, 1526–1530.

65. Tamura, K., Peterson, D., Peterson, N., Stecher, G., Nei, M., and Kumar, S. (2011). MEGA5: molecular evolutionary genetics analysis using maximum likelihood, evolutionary distance, and maximum parsimony methods. Mol. Biol. Evol. *28*, 2731–2739.

66. Yang, X., Ma, N., Yang, L., Zheng, Y., Zhen, Z., Li, Q., Xie, M., Li, J., Zhang, K.Q., and Yang, J. (2018). Two Rab GTPases play different roles in conidiation, trap formation, stress resistance, and virulence in the nematode-trapping fungus *Arthrobotrys oligospora*. Appl. Microbiol. Biotechnol. *102*, 4601–4613.

67. Colot, H.V., Park, G., Turner, G.E., Ringelberg, C., Crew, C.M., Litvinkova, L., Weiss, R.L., Borkovich, K.A., and Dunlap, J.C. (2006). A high-throughput gene knockout procedure for *Neurospora* reveals functions for multiple transcription factors. Proc. Natl. Acad. Sci. USA *103*, 10352–10357.

68. Shao, W., Cai, Q., Tong, S.M., Ying, S.H., and Feng, M.G. (2020). Nuclear Ssr4 is required for the in vitro and in vivo asexual cycles and global gene activity of *Beauveria bassiana*. mSystems *5*, e00677-19.

69. Dong, X., Si, J., Zhang, G., Shen, Z., Zhang, L., Sheng, K., Wang, J., Kong, X., Zha, X., and Wang, Y. (2021). The role of Jacalin-related lectin gene AOL_s00083g511 in the development and pathogenicity of the nematophagous fungus *Arthrobotrys oligospora*. J. Microbiol. *59*, 736–745.

70. Tunlid, A., Ahman, J., and Oliver, R.P. (1999). Transformation of the nematode-trapping fungus *Arthrobotrys oligospora*. FEMS Microbiol. Lett. *173*, 111–116.

71. Zhou, D., Zhu, Y., Bai, N., Yang, L., Xie, M., Yang, J., Zhu, M., Zhang, K.Q., and Yang, J. (2022). *AoATG5* plays pleiotropic roles in vegetative growth, cell nucleus development, conidiation, and virulence in the nematode-trapping fungus *Arthrobotrys oligospora*. Sci. China Life Sci. *65*, 412–425.

72. Jiang, K.X., Liu, Q.Q., Bai, N., Zhu, M.C., Zhang, K.Q., and Yang, J.K. (2022). AoSsk1, a response regulator required for mycelial growth and development, stress responses, trap formation, and the secondary metabolism in *Arthrobotrys oligospora*. J. Fungi *8*, 260.

73. Ma, Y., Yang, X., Xie, M., Zhang, G., Yang, L., Bai, N., Zhao, Y., Li, D., Zhang, K.Q., and Yang, J. (2020). The Arf-GAP AoGlo3 regulates conidiation, endocytosis, and pathogenicity in the nematode-trapping fungus *Arthrobotrys oligospora*. Fungal Genet. Biol. *138*, 103352.

74. Li, X., Zhu, M., Liu, Y., Yang, L., and Yang, J. (2023). *Aoatg11* and *Aoatg33* are indispensable for mitophagy, and contribute to conidiation, the stress response, and pathogenicity in the nematode-trapping fungus *Arthrobotrys oligospora*. Microbiol. Res. *266*, 127252.

STAR★METHODS

KEY RESOURCES TABLE

REAGENT or RESOURCE	SOURCE	IDENTIFIER
Bacterial and virus strains		
Escherichia coli DH5a	Takara	Cat#9057
Chemicals, peptides, and recombinant proteins		
Tryptone	OXOID	Cat#LP0042B
Yeast extract	OXOID	Cat#LP0021B
Molasses	Solarbio	Cat#FA0070
Sorbitol	Solarbio	Cat#S8090
NaCl	Solarbio	Cat#S8210
SDS	Solarbio	Cat#S8010
Congo red	Solarbio	Cat#C8450
Menadione	Sigma	Cat#M5750-25G
Sucrose	Solarbio	Cat#S8271
Calcofluor white (CFW)	Sigma	Cat#910090
4',6-diamidino-2-phenylindole (DAPI)	Sigma	Cat#D9524
FM4-64	Biotium	Cat#70021
Critical commercial assays		
one-step TUNEL apoptosis detection kit	Beyotime	Cat#C1086
PrimeScriptH^{RT} reagent kit	Takara	Cat#RR037A
LightCycler 480 SYBR Green I Master	Roche	Cat#4887352001
Experimental models: Organisms/strains		
Arthrobotrys oligospora	ATCC	ATCC: 24927
Δ*fus3* mutant strains generated in this study	This paper	N/A
Caenorhabditis elegans	CGMCC	N2
Deposited data		
Transcriptomic data	This paper	GSE212172
Oligonucleotides		
For all oligonucleotides used for gene manipulation and RT-qPCR	See Table S1	N/A
Software and algorithms		
pI/MW tool	Expasy	http://web.expasy.org/compute_pi/
InterProScan		http://www.ebi.ac.uk/Tools/pfa/iprscan/
DNAman	Lynnon Biosoft	https://www.lynnon.com/qa.html
MEGA 5	Tamura et al.[65]	https://www.megasoftware.net/
ImageJ	Schneider et al., 2012	https://imagej.net/Welcome
Prism 5	GraphPad Software	https://www.graphpad.com/
STRING	Hao et al.[37]	https://cn.string-db.org/
Cytoscape	Franz et al.[38]	https://cytoscape.org/

RESOURCE AVAILABILITY

Lead contact

Further information and requests for resources and reagent should be directed to and will be fulfilled by the Lead Contact, Jinkui Yang (jinkui960@ynu.edu.cn).

Materials availability

This study did not generate new unique reagents.

Data and code availability

- Data: All data and methods necessary to reproduce this study are included in the manuscript and Supplemental Information. Sequencing data were deposited to the National Center for Biotechnology Information under accession number GSE212172 and are publicly available.
- Code: This paper does not report original code.
- Other items: Any additional information required to reanalyze the data reported in this paper is available from the lead contact upon request.

EXPERIMENTAL MODEL AND STUDY PARTICIPANT DETAILS

Fungal strains

The WT strain *A. oligospora* (ATCC24927) and two positive transformant (Δ*fus3*-71 and Δ*fus3*-72) strains were routinely incubated on PDA medium at 28°C. Fungal strains were cultured at 28°C on PDA, TG, and TYGA media for mycelial growth analysis as previously described.[20,66] The *S. cerevisiae* FY834 strain (ATCC90845), as a host of recombinant plasmid vector, was cultured with yeast extract–peptone–glucose (YPD) medium.

Bacterial strain

Escherichia coli DH5α strains carrying pRS426 and pCSN44 plasmids (TaKaRa, Japan) were cultured in Luria-Bertani broth agar supplemented with 50 μg/mL kanamycin or 100 μg/mL ampicillin, respectively.

Nematode

The *Caenorhabditis elegans* used to induce trap formation in the bioassays were incubated on oat medium.[42]

METHOD DETAILS

Sequence analysis of Fus3

The sequences of Fus3 (GenBank: AOL_s00110g154) were retrieved on the basis of the homologous sequences of the model fungi *S. cerevisiae* (GenBank: AAA34613) and *M. oryzae* (GenBank: XP_003712175) using BLAST searches in the NCBI database (https://www.ncbi.nlm.nih.gov/). The theoretical isoelectric point (pI) and molecular mass of Fus3 were analyzed by the pI/MW tool (http://www.expasy.ch/tools/pi_tool.html). Sixteen orthologous Fus3 were retrieved from different fungi in the NCBI database, the structural domains of the homologs of Fus3 were analyzed on the Pfam website (http://pfam.xfam.org/), and the sequence similarity between Fus3 and other orthologs was compared using DNAman software (version 5.2.2). A phylogenetic tree was constructed using MEGA software (version 5) with the neighbor-joining method.[65]

Deletion of fus3

Disruption of the *fus3* gene was performed using the homologous recombination method as previously described.[67] The 5′- and 3′-flanking regions of the *fus3* gene (2,064 and 1,927 bp) and the hygromycin resistance cassette (*hph*) were individually amplified by PCR with paired primers (Table S1). The three DNA fragments were isolated using a PCR product recovery kit (TaKaRa) and then co-transformed into the *S. cerevisiae* FY834 strain by electroporation[68,69] with linearized pRS426 (digested with *Eco*RI and *Xho*I) to generate the pRS426-*fus3*-*hph* recombinant plasmid. Complete disruption sequences were amplified using primers *fus3*-5f/*fus3*-3r (Table S1) and transformed into *A. oligospora* protoplasts as previously described.[66,69] Then, positive transformants grown on PADS medium were verified by PCR and Southern blotting.[70] Genomic DNA of the WT and Δ*fus3* mutant strains were extracted using a plant genomic DNA Kit (TaKaRa) and digested using *Stu*I for Southern blotting analysis.

Analysis of vegetative growth, morphogenesis, and conidiation

To analyze mycelial growth, WT and Δ*fus3* mutant strains were cultured on PDA, TYGA, and TG agar plates at 28°C for 7 days.[20] To determine the spore yield for each strain, they were assayed as previously described

after 15 days post inoculation (dpi) in corn meal yeast extract (CMY) medium.[71,72] Freshly harvested hyphae and spores were stained with 20 μg/mL calcofluor white (CFW) (Sigma-Aldrich, USA) to visualize their morphology and hyphal fusion, and 20 μg/mL 4',6-diamidino-2-phenylindole (DAPI) (Sigma-Aldrich, USA) to visualize their nuclei. Samples were all observed and photographed with an inverted fluorescence microscope (DS-Ri2, Nikon, Tokyo, Japan).

To observe endocytosis, sterile coverslips were inserted into WT and Δ*fus3* mutant strains in PDA medium at 28°C for 7 days, and then the coverslips covered with hyphae were stained with the lipophilic dye FM4-64 was diluted 40 times (Biotium, California, USA) for 1 min and 10 min, respectively.[73] The ultrastructures of the mycelium, conidia, and traps were observed using TEM and SEM, and the samples were prepared as previously described.[30,42] To observe apoptosis, hyphal coverslip inserts were cultured on a CMY plate (9 cm) at 28°C for 7 days; then, the coverslips covered with hyphae stained with one-step terminal deoxynucleotidyl transferase dUTP nick end labeling (TUNEL, 30 μg/mL) assay solution (Beyotime Biotechnology, Haimen, China) at 37°C for 30 min, followed by 20 mg/mL DAPI for 30 min at room temperature.

Stress assays

WT and Δ*fus3* mutant strains were cultured on TG medium alone (control) or TG medium supplemented with chemical stressors for 7 days at 28°C to measure responses to chemical stressors. The chemical stressors were oxidants (H_2O_2 and menadione), cell wall-perturbing agents (SDS and Congo red), and osmotic agents (NaCl and sorbitol). The diameter of the colony was measured on day 7, and the relative growth inhibition (RGI) values of the fungal colonies under stress were calculated using the equation (Sc − St)/(Sc − d) × 100, where Sc and St denote the areas of the stressed and unstressed (control) colonies, respectively, and d is the constant area of the hyphal mass discs used to initiate colonies.[31]

Trap formation and morphogenesis

Equal amounts of fresh spores of WT and Δ*fus3* mutants were evenly spread on the water agar WA plate (6 cm) at 28°C for 3 days. Then, approximately 300 *C. elegans* were added to each plate for trap induction. The numbers of traps and nematodes captured in each plate were then observed and counted under a light microscopy (Olympus, Tokyo, Japan) every 12 h until 48 h. Three replicates were used for each experiment.

Transcriptome sequencing and analysis

WT and Δ*fus3* strains were grown on cellophane-overlaid PDA plates at 28°C for 5 days. Approximately 600 nematodes were then added to each plate for 0, 12, 24, and 36 h of induction, and three replicates were used for each sample. After collecting the samples, RNA was extracted with the AxyPrep multisource RNA miniprep Kit (Axygen, Jiangsu, China), and then sent to Majorbio Bio-Pharm Technology Co., Ltd. (Shanghai, China) for transcriptome sequencing. The final cDNA library was sequenced on an Illumina Novaseq 4000 platform. The clean reads were mapped to the *A. oligospora* (ATCC 24927) genome sequence. The gene expression changes were evaluated and the DEGs were identified with an FDR value of $\leq$0.05. High-throughput sequencing data were analyzed using the OmicShare online platform (www.majorbio.com).

LC-MS assay

WT and Δ*fus3* strains were inoculated into PD broth for 7 days at 28°C; then, mycelium and fermentation broth were separated by filtration using a vacuum filter pump. The isolated mycelium was further dried and weighed, and corresponding fermentation broth was prepared according to the same weight of the mycelium. The fermentation broth was added to an equal volume of ethyl acetate and left to stand for extraction for 12 h, and then the crude extract obtained using a rotary evaporator was dissolved in 1 mL of methanol.[74] Extracts were used for subsequent LC-MS (Thermo Scientific Ultimate 3000, Thermo Fisher Scientific, USA) analysis. Metabolic profiles and untargeted metabolomics of WT and Δ*fus3* mutant strains were analyzed using Thermo Xcalibur software and Compounds Discoverer 3.0 software (Thermo Fisher Scientific), respectively.

RT-qPCR analysis

WT and Δ*fus3* strains were cultured on TYGA at 28°C for 3, 5, or 7 days, and total RNA from mycelium was extracted with AxyPrep multisource RNA miniprep kit, and then translated into cDNA a FastQuant RT kit with gDNase (TaKaRa).The cDNA was further used as a template for RT-qPCR using SYBR Premix Ex

TaqTM (TaKaRa) and specific primers (Table S1) to detect the transcript levels of candidate genes related to conidiation, cell wall biosynthesis, and oxidative stress response; the β-tubulin-encoding gene was used as an internal standard. The mRNA level was analyzed using the $2^{-\Delta\Delta Ct}$ method.[51]

Y2H screening

The CDS regions of *fus3*, *pyp1*, *ste12*, and *flbA* were amplified from total cDNA using specific primers (Table S1) and inserted into pGADT7-AD and pGBKT7-BD vectors. The constructed plasmids were sequenced at Tsingke Biotechnology Co., Ltd. (Beijing, China). Then, the constructed vector was co-transformed into *S. cerevisiae* strain AH109 using the LiAc/SS-DNA/PEG transformation protocol (TaKaRa, Dalian, China), and further cultured on synthetic defined (SD) medium without Trp and Leu at 30°C for 3–5 days. Finally, self-activation or interaction was screened by SD/-Trp/-Leu/-His/-Ade and SD/-Trp/-Leu/-His/-Ade/+AbA/+X-α-Gal plates.

Analysis of regulatory network of Fus3

Based on the transcriptome analysis between the WT and Δ*fus3* mutant strains, several genes related to remarkably enriched GO terms were selected, including cell communication-, basal transcription factor-, cell cycle-, translation-, cell response to stress-, nutrient metabolism-, and sporulation-related genes, as well as several genes that have been reported to interact with Fus3, such as Far11-, Cdc24-, and Cdc42-related genes.[3,13] The network of Fus3 and its putative target genes were analyzed using STRING[37] and then mapped using Cytoscape version 3.9.0.[38] String ID and annotation of each target gene in the network are listed in Table S10.

QUANTIFICATION AND STATISTICAL ANALYSIS

Each experiment was conducted with three parallel replicates, and the data were shown as mean ± standard deviation (SD). One-way analysis of variance (ANOVA) was applied in statistical analysis of multiple measurements for all strains, and the significance was determined by Tukey's honest significance test (Tukey's HSD). P value < 0.05 was considered significant. Statistical analyses were performed with the software of GraphPad Prism 8 (GraphPad Software, San Diego, CA, USA).